

Semidefinite programming for understanding limitations of Lindblad equations

Soumyadeep Sarma,^{1, 2, *} Manas Kulkarni,^{2, †} Archak Purkayastha,^{3, ‡} and Devashish Tupkary^{4, §}

¹*Indian Institute of Science, Bangalore 560012, India*

²*International Centre for Theoretical Sciences, Tata Institute of Fundamental Research, Bangalore 560089, India*

³*Department of Physics, Indian Institute of Technology, Hyderabad 502284, India*

⁴*Institute for Quantum Computing and Department of Physics and Astronomy,
University of Waterloo, Waterloo, Ontario, Canada, N2L 3G1*

(Dated: February 3, 2026)

Lindbladian quantum master equations (LEs) are the most popular descriptions for quantum systems weakly coupled to baths. But, recent works have established that in many situations such Markovian descriptions are fundamentally limited: they cannot simultaneously capture populations and coherences even to the leading-order in system-bath couplings. This can cause violation of fundamental properties like thermalization and continuity equations associated with local conservation laws, even when such properties are expected in the actual setting. This begs the question: given a physical situation, how do we know if there exists an LE that describes it to a desired accuracy? Here we show that, for both equilibrium and non-equilibrium steady states (NESS), this question can be succinctly formulated as a semidefinite program (SDP), a convex optimization technique. If a solution to the SDP can be found to a desired accuracy, then an LE description is possible for the chosen setting. If not, no LE description is fundamentally attainable, showing that a consistent Markovian treatment is impossible even at weak system-bath coupling for that particular setting. Considering few qubit isotropic XXZ-type models coupled to multiple baths, we find that in most parameter regimes, LE description giving accurate populations and coherences to leading-order is unattainable, leading to rigorous no-go results. However, in some cases, LE description having correct populations but inaccurate coherences, and satisfying local conservation laws, is possible over some of the parameter regimes. Our work highlights the power of semidefinite programming in the analysis of physically consistent LEs, thereby, in understanding the limits of Markovian descriptions at weak system-bath couplings.

I. INTRODUCTION

Lindblad quantum master equations —With the advent of quantum technology, accurately describing small quantum systems out of equilibrium has become paramount. However, this is a challenging theoretical problem in general, even when the number of degrees of freedom in the system is small. Consequently, several approximations are very often required [1–5]. One of the most common approximations, which greatly simplifies such descriptions, is to assume that the dissipative dynamics of the system is Markovian. Indeed Markovian quantum master equations form the backbone of much of modern open quantum system dynamics, capturing the evolution of systems coupled to external baths in both equilibrium and non-equilibrium conditions [1–5], as well as shaping our understanding of how quantum measurements are performed in practice [6–11]. It was shown by Gorini, Kossakowski, Sudarshan, and Lindblad (GKSL) [12, 13] that any quantum master equation that preserves complete positivity and trace of the density matrix, and describes Markovian dynamics with no explicit

time-dependence has to be of the form

$$\begin{aligned} \frac{\partial \rho}{\partial t} &= i[\rho, H_S + H_{LS}] + \mathcal{D}(\rho), \\ \mathcal{D}(\rho) &= \sum_{\lambda=1}^{d^2-1} \gamma_\lambda \left(L_\lambda \rho L_\lambda^\dagger - \frac{1}{2} \{L_\lambda^\dagger L_\lambda, \rho\} \right), \quad \gamma_\lambda \geq 0, \end{aligned} \quad (1)$$

which is commonly called the Lindblad quantum master equation (LE). In Eq. (1), ρ is the density matrix of the system, d is the Hilbert space dimension of the system, H_S is the system Hamiltonian, H_{LS} is the so-called Lamb shift Hamiltonian, L_λ are the Lindblad operators, γ_λ are the rates, and $\mathcal{D}(\rho)$ is called the “dissipator” term. The preservation of complete positivity condition is enforced by demanding $\gamma_\lambda \geq 0$. Within the Markovian regime, the GKSL framework [12, 13] guarantees complete positivity and trace preservation (CPTP), ensuring physical consistency.

Born-Markov approximation and Redfield equation —However, Eq.(1) only gives the mathematical form of the Markovian quantum master equation. The Hamiltonians, the Lindblad operators and the rates need to be found based on the physical situation to be described. In practice, the system Hamiltonian may be known, but at best partial information is available for the baths, like their spectral functions, and thermodynamic properties like temperatures and chemical potentials. Given such physical situations, it becomes important to find conditions under which Eq. (1) may be obtained.

* ssoumyadeep@iisc.ac.in

† manas.kulkarni@icts.res.in

‡ archak.p@phy.iith.ac.in

§ djupkary@uwaterloo.ca

The most standard and general way to arrive at Markovian quantum master equations in such microscopic approach is via the Born-Markov approximation [1–5]. This relies on weak system-bath couplings and a time-scale separation between system and the baths, obtaining a quantum master equation to leading-order in system-bath coupling. The quantum master equation obtained is of the so-called Bloch-Redfield form [14, 15], commonly called Redfield equation (RE). The RE can be cast into the form of the LE [Eq. (1)], with one major caveat. It can be shown in generality that, unless in very special situations, one or more of the rates, γ_λ , will be negative [16–19]. This violates the complete positivity requirement. So, time evolution by RE may cause the density matrix ρ to have unphysical negative eigenvalues. To alleviate this issue, various further approximations are often performed to make the rates positive, leading to various forms of LE [20–33].

The LE versus RE conundrum — Despite not having complete positivity, remarkably, the RE has been rigorously shown to give both populations (diagonal elements of ρ in eigenbasis of H_S) and coherences (off-diagonal elements of ρ in eigenbasis of H_S) correctly to leading-order in system-bath couplings [34, 35]. As a consequence, the RE has been shown to perfectly satisfy local conservation laws of the actual physical situation and capture thermalization when that is physically expected [34].

Contrarily, it has been recently argued rigorously that most further approximations to re-establish complete positivity will lead to inaccurate populations or coherences even in the leading-order. This can cause violation of continuity equations related to local conservation laws and of thermalization, even when such properties are expected in the actual physical situation [34].

This leads to a conundrum. It shows that even at weak system-bath coupling, a consistent Markovian quantum master equation description, which can accurately give the density matrix to the leading-order in system-bath coupling, is hard to find in most situations. One is forced to either choose RE, giving up complete positivity, or choose one of the forms of LE, allowing violation of some fundamental properties and inaccuracies in the density matrix even to the leading-order.

Present paper: semidefinite program to check for possible LE — The above general discussion leads to the following question: given a physical situation, how do we know if an LE description with desired accuracy is attainable that does not violate any fundamental property of the setting? The fact that there are various different approximation schemes to recover an LE from RE [20–33] makes answering this question difficult, especially when the answer is negative. For a given physical setting, even if several approximation schemes have been tried and none satisfy the desired requirements, one cannot easily rule out the possibility of an improved approximation scheme which meets all requirements for a consistent Markovian description.

In the present paper, we seek to address this. For

non-degenerate finite-dimensional system Hamiltonians, and in absence of any explicit time-dependent drive, we provide a numerical technique which can rigorously show whether a consistent LE description of a non-equilibrium steady state (NESS) is possible for a given physical situation, up to a chosen accuracy. We do so by showing that the above question can be formulated as a convex optimization problem in the form of a semidefinite program (SDP) [36]. The SDP can be solved using standard packages in high-level programming languages. Crucially, when the resulting optimization problem takes the form of a semidefinite program (SDP), its well-understood duality structure allows one to obtain rigorous and tight bounds on the optimal value, thereby providing definitive statements about whether the desired properties can be achieved up to a prescribed tolerance. If a solution can be found to a desired accuracy, then an LE description may be possible. Standard solvers also output one candidate for such an LE. If the SDP does not have a solution to our desired accuracy, an LE description is fundamentally unattainable, thereby giving a rigorous no-go result for any Markovian description of that physical setting. Such a fundamental lack of Markovian description means the dynamics necessarily have some non-Markovian features.

Even if there is no LE possible that correctly gives both populations and coherences to leading-order, an LE giving only correct populations and incorrect coherences (thereby having leading-order inaccuracies in density matrix) may still be possible. We show that such LEs can also be searched for by casting the problem into a slightly different SDP.

We remark here that while SDPs are widely used in quantum information and communication, only few previous works have used it for open quantum system descriptions [19, 37–39]. In Ref. 37, the problem of assessing non-Markovianity of a quantum channel was converted into an SDP, while in Ref. 19, some of the present authors formulated the problem of searching for LEs showing thermalization and satisfying local conservation laws into an SDP. Our present results stem from combining the ideas in Ref. 19 with the fact the RE gives NESS populations and coherences in energy eigenbasis correctly to the leading-order [34, 35]. One major difference is that in this work we study both equilibrium and non-equilibrium settings, and investigate a broader class of scenarios. This builds on and utilizes the results of Ref. 19, which focused exclusively on the equilibrium case.

We exemplify our methods by applying to few-qubit isotropic XXZ-type chains coupled to multiple baths. Below we summarize our results in this regard.

1. *First and last qubits attached to baths at finite temperatures:* In this case, LE description is fundamentally unattainable across all system parameter regimes. This is true at equilibrium (both baths having same temperature), as well as at NESS (both baths having different temperatures). It is even impossible to have an LE description hav-

ing only correct populations (incorrect coherences) to leading-order and satisfying local conservation laws.

2. *First two and last two qubits attached to baths at finite temperatures:* In this case also, LE description is fundamentally unattainable across all parameter regimes. However, when all qubits are identical, and the coupling between qubits is relatively low, an LE description giving only correct steady-state populations (but incorrect coherences) and satisfying local conservation laws is possible. This is also true both in equilibrium (i.e. when all baths have same temperature) and in NESS.
3. *Finite temperature baths attached at all the qubits:* In the equilibrium case in this setting, a physically consistent LE is attainable. However, at NESS, when temperature of even one bath is different, or even one site is detached from a bath, LE description is unattainable.

The above gives rigorous no-go results for Markovian description of steady-state of dissipative isotropic XXZ-type qubit chains, even when the baths are weakly coupled.

The remainder of the paper is structured as follows: In Sec. II, we explain the system and heat bath models focusing on the general requirements in Markovian QME and how the metrics defined as τ^{pop} and $\tau^{\text{pop,coh}}$ can be formulated as convex optimization problems. We also highlight our analytically calculated lower bound on the trace distance between the exact NESS and the NESS obtained from any LE. In Sec. III, we present the main numerical results of our optimized metrics plotted over a large parameter regime summarised in the form of Table I and discuss the differences between cases of attaching one and two qubits to the left and right baths. We also present numerical data and discuss how attaching all qubits to baths in equilibrium leads to a NESS with correct leading-order populations and coherences. We conclude with a summary and outlook in Sec. IV and delegate important technical details to the appendices.

II. MODEL DESCRIPTION AND STEADY-STATE REQUIREMENTS IN MARKOVIAN QMES

In this section, we start with a description of our system and then discuss the conditions for obtaining the correct populations and coherences of the steady state density matrix, both in and out of equilibrium. We investigate this under Redfield formalism and for a general LE satisfying complete positivity and trace preservation along with local conservation laws. Finally, we formulate these as optimization problems under the paradigm of semidefinite programming (SDP).

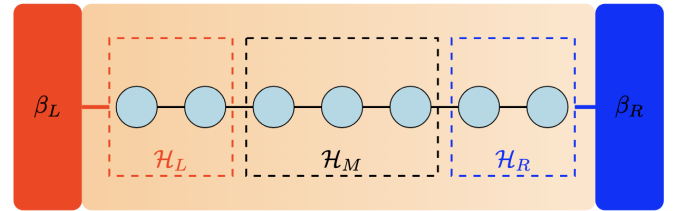


FIG. 1. Schematic of an arbitrary finite-dimensional system described by Hamiltonian H_S [Eq. (3)], parts of which are weakly coupled to left and right thermal baths [Eq. (4)] at inverse temperatures β_L and β_R . The Hilbert space of the system, \mathcal{H}_S , is divided into parts \mathcal{H}_L (which directly couples to the Hilbert space of the left bath), \mathcal{H}_R (which directly couples to the Hilbert space of the right bath), and the remaining part \mathcal{H}_M .

A. System and heat bath description

Here, we set up our model which is similar to the model presented in Ref. 19. We consider the following generic system-bath setup. Let us denote \mathcal{H}_L (\mathcal{H}_R) as the Hilbert space of the part of the system that connects to the left (right) bath and let \mathcal{H}_M be the Hilbert space of the remaining part of the system. The Hamiltonian H of the full setup including the system and all the baths is (cf. Fig. 1)

$$H = H_S + \epsilon H_{SB} + H_B, \quad (2)$$

$$H_S = H_L + H_{LM} + H_M + H_{RM} + H_R, \quad (3)$$

$$H_B = H_B^L + H_B^R. \quad (4)$$

Here H_B is the composite Hamiltonian of all the baths, composed of Hamiltonian for the left (H_B^L) and right (H_B^R) baths with inverse temperatures β_L and β_R respectively. H_{SB} is the composite Hamiltonian describing system-bath coupling to all the baths and $\epsilon \ll 1$ is a dimensionless parameter that controls the strength of system-bath coupling. The Hamiltonian H_L (H_R) acts on the Hilbert space \mathcal{H}_L (\mathcal{H}_R), the Hamiltonian H_M on the Hilbert space \mathcal{H}_M , and H_{LM} (H_{RM}) on both Hilbert spaces \mathcal{H}_L (\mathcal{H}_R) and \mathcal{H}_M .

The initial state of the full set-up is taken as $\rho_{\text{tot}}(0) = \rho(0) \otimes \rho_B$, where $\rho(0)$ is the initial state of the system and ρ_B is the composite state of all the baths. Without loss of generality, it is possible to assume that $\text{Tr}(H_{SB} \rho(0) \otimes \rho_B) = 0$ [1]. The state of the system at a time t is

$$\rho(t) = \text{Tr}_B (e^{-iHt} \rho(0) \otimes \rho_B e^{iHt}), \quad (5)$$

where $\text{Tr}_B(\dots)$ implies trace over bath degrees of freedom. Notice that Eq. (5), by construction, is a CPTP map from $\rho(0)$ to $\rho(t)$ [1, 40]. We will assume that in the long-time limit, the system reaches a unique NESS. This assumption physically necessitates that the system size is finite while the baths are in the thermodynamic limit. For simplicity, we will further assume that there are no

degeneracies in H_S . This prevents coherences from possibly having $\mathcal{O}(1)$ contributions. We shall see later that leading-order contributions for coherences is $\mathcal{O}(\epsilon^2)$. The NESS density matrix is then defined as

$$\rho_{\text{NESS}} = \lim_{t \rightarrow \infty} \text{Tr}_B (e^{-iHt} \rho(0) \otimes \rho_B e^{iHt}). \quad (6)$$

It is possible to expand the NESS density matrix in powers of ϵ . Owing to the previously mentioned assumption that $\text{Tr}(H_{SB} \rho(0) \otimes \rho_B) = 0$, it can be shown that, only even powers of ϵ can feature in any such expansion [Sec. 3.3 of Ref. 1]. Hence we have,

$$\rho_{\text{NESS}} = \sum_{m=0}^{\infty} \epsilon^{2m} \rho_{\text{NESS}}^{(2m)}, \quad (7)$$

where $\rho_{\text{NESS}}^{(2m)}$ stands for the order-by-order NESS density matrix. The QME describing the evolution of $\rho(t)$ in the long-time limit can also be expanded in the so-called time-convolution-less (TCL) form [Sec.(9.2.2) of Ref. 1]. Such an expansion from Eq. (7), up to some arbitrary high-order, can be formally written as

$$\frac{\partial \rho}{\partial t} = \sum_{m=0}^{\infty} \epsilon^{2m} \mathcal{L}_{2m}[\rho(t)]. \quad (8)$$

In Eq. (8), for $m = 0$, we have that:

$$\mathcal{L}_0[\rho(t)] = i[\rho(t), H_S]. \quad (9)$$

The higher order superoperators $\mathcal{L}_{2m}[\rho(t)]$ that appear in Eq. (8) are more complicated and there is a systematic way to obtain them. Because the QME must be a linear equation, each superoperator appearing in the above expansion is linear. Since, ρ_{NESS} is the long-time steady-state, by definition, it satisfies

$$0 = \sum_{m=0}^{\infty} \epsilon^{2m} \mathcal{L}_{2m}[\rho_{\text{NESS}}]. \quad (10)$$

Using the expression for ρ_{NESS} from Eq. (7), we can now analyze and solve Eq. (10) in an order-by-order manner in the discussion that follows.

B. Solving for the exact steady-state

Let d be the dimension of the Hilbert space. Thus ρ is a $d \times d$ matrix. Taking the $\epsilon \rightarrow 0$ limit of Eq. (10) yields, in combination with Eq. (7),

$$\mathcal{L}_0[\rho_{\text{NESS}}^{(0)}] = [\rho_{\text{NESS}}^{(0)}, H_S] = 0. \quad (11)$$

Here $H_S = \sum_{\alpha} E_{\alpha} |E_{\alpha}\rangle \langle E_{\alpha}|$ is a spectral decomposition in the energy eigenbasis $\{|E_{\alpha}\rangle\}$. This implies that $\rho_{\text{NESS}}^{(0)}$ is diagonal in the energy eigenbasis of the system,

$$\langle E_{\alpha} | \rho_{\text{NESS}}^{(0)} | E_{\nu} \rangle = 0 \quad \forall \alpha \neq \nu, \quad (12)$$

Thus,

$$\rho_{\text{NESS}}^{(0)} = \sum_{\alpha} p_{\alpha} |E_{\alpha}\rangle \langle E_{\alpha}|. \quad (13)$$

The next set of equations on comparing the second-order terms in ϵ (i.e. ϵ^2) in Eq. (10) is given by

$$\langle E_{\alpha} | \mathcal{L}_2[\rho_{\text{NESS}}^{(0)}] | E_{\alpha} \rangle = 0 \quad \forall \alpha. \quad (14)$$

This fixes the diagonal values of $\rho_{\text{NESS}}^{(0)}$, i.e, it fixes the values of p_{α} . Note that there are d equations and d variables, and therefore the set of equations uniquely determine the values of the p_{α} . Similarly, at order ϵ^2 , from Eq. (10), we have for off-diagonal elements

$$i(E_{\alpha} - E_{\nu}) \langle E_{\alpha} | \rho_{\text{NESS}}^{(2)} | E_{\nu} \rangle + \langle E_{\alpha} | \mathcal{L}_2[\rho_{\text{NESS}}^{(0)}] | E_{\nu} \rangle = 0, \quad (15)$$

which holds for $\forall \alpha \neq \nu$. This fixes the off-diagonal values of $\rho_{\text{NESS}}^{(2)}$ given $E_{\alpha} \neq E_{\nu}$ when $\alpha \neq \nu$ (i.e. no degeneracies). Note that since there are $d^2 - d$ equations and $d^2 - d$ variables, the set of equations uniquely determine the solutions. Finally, at order ϵ^4 in Eq. (10) for diagonal elements, we have

$$\langle E_{\alpha} | \mathcal{L}_2[\rho_{\text{NESS}}^{(2)}] | E_{\alpha} \rangle + \langle E_{\alpha} | \mathcal{L}_4[\rho_{\text{NESS}}^{(0)}] | E_{\alpha} \rangle = 0, \quad (16)$$

which fixes the diagonal values of $\rho_{\text{NESS}}^{(2)}$. All properties discussed above correspond to the exact NESS, obtained in the regime of small ϵ . Most often, higher-order terms are very difficult to treat. Therefore the QME only up to the leading-order term in ϵ , that is ϵ^2 , is considered.

C. Redfield formalism and physical consistency

To arrive at the Redfield master equation (RE), we take the composite state of all baths $\rho_B \equiv \rho_B^L \otimes \rho_B^R$ to be the thermal state.

$$\rho_B^i = \frac{e^{-\beta_i H_B^i}}{Z_B^i}, \quad i = L, R. \quad (17)$$

Without any loss of generality, we assume $\text{Tr}_B(H_{SB} \rho(0) \otimes \rho_B) = 0$ [1, 40]. The RE equation is the full expansion in Eq. (8) truncated to second order in ϵ (i.e. up to ϵ^2) and is given by

$$\frac{\partial \rho}{\partial t} = \mathcal{L}_0[\rho(t)] + \epsilon^2 \mathcal{L}_2[\rho(t)]. \quad (18)$$

Here recall from Eq. (9) that $\mathcal{L}_0[\rho(t)] = i[\rho(t), H_S]$ and \mathcal{L}_2 is given by [1],

$$\mathcal{L}_2[\rho(t)] = \int_0^{\infty} dt' \text{Tr}_B[H_{SB}, [H_{SB}(t - t'), \rho(t) \otimes \rho_B]]. \quad (19)$$

where

$$H_{SB}(t) = e^{i(H_S + H_B)t} H_S B e^{-i(H_S + H_B)t}. \quad (20)$$

Even though a CPTP map gives the actual microscopic evolution [see Eq. (5)], the microscopically derived RE violates complete positivity unless in extremely special cases such as rapidly oscillating off-diagonal terms in the interaction picture [1], positive semi-definite Redfield tensor [41], single qubit weakly interacting with bath [42]. Repeating the same analysis as in section II B, we find that since only \mathcal{L}_0 and \mathcal{L}_2 show up in Eqs. (11) to (15), the zeroth-order RE NESS is the same as the exact zeroth-order NESS, and the coherences of second-order RE NESS are the same as the coherences of the second-order exact NESS (recall that for coherences, the second-order is the leading order).

However, note that diagonal values of $\rho_{\text{NESS}}^{(2)}$ will deviate from the second-order NESS of the exact case, since RE does not have an analogue of the exact Eq. (16) (we omitted \mathcal{L}_4). Let us now understand how we can utilize $\rho_{\text{NESS}}^{(0)}$ to search for LEs having NESS with correct leading-order populations (from $\rho_{\text{NESS}}^{(0)}$) and/or coherences (from $\rho_{\text{NESS}}^{(2)}$).

D. Requirements in a Markovian QME

Let us look at some conditions which one might possibly require for a generic Markovian QME, given as

$$\frac{\partial \bar{\rho}}{\partial t} = \mathcal{L}_0[\bar{\rho}(t)] + \epsilon^2 \mathcal{L}'_2[\bar{\rho}(t)], \quad (21)$$

where we replace \mathcal{L}_2 of RE with \mathcal{L}'_2 of any other QME. We use $\bar{\rho}$ to denote the system density matrix obtained via this QME, in contrast to ρ for the RE system density matrix.

1. The CPTP condition

First, we wish to preserve complete positivity and trace (CPTP map) for which one requires a Lindbladian form as given in Eq. (1). This means that \mathcal{L}'_2 present in Eq. (21) has to have a Lindbladian form [Eq. (1)].

2. Local conservation laws

Second, for physical consistency, we require local conservation laws. For this, consider the dynamical equation for the expectation value of any observable O_M on \mathcal{H}_M [see Fig. 1], which is given by

$$\frac{d}{dt} \langle I_L \otimes O_M \otimes I_R \rangle = -i \langle [I_L \otimes O_M \otimes I_R, H_S] \rangle, \quad (22)$$

where $\langle X \rangle = \text{Tr}[X \rho]$. Any effective QME obtained by integrating out the bath should satisfy this property. We call QMEs satisfying this property [Eq. (22)] as ones preserving local conservation laws. The most general form of Markovian QME respecting the restrictions for satisfying complete positivity [Eq. (1)] and local conservation laws [Eq. (22)] was shown in Ref. 19 to be one where the Lindblad operators and the Lamb Shift Hamiltonian only act on the part of the system connected to the bath, and are identity elsewhere. Thus, it is given by

$$\begin{aligned} \frac{\partial \bar{\rho}}{\partial t} = & i[\bar{\rho}, H_S + \epsilon^2 H_{LS}^{(L)} \otimes I_{MR} + \epsilon^2 I_{LM} \otimes H_{LS}^{(R)}] \\ & + \epsilon^2 \sum_{\alpha_L, \tilde{\alpha}_L=1}^{d_L^2-1} \Gamma_{\alpha_L, \tilde{\alpha}_L}^{(L)} \left(\left(f_{\tilde{\alpha}_L} \otimes \frac{I_{MR}}{\sqrt{d_M d_R}} \right) \bar{\rho} \left(f_{\alpha_L} \otimes \frac{I_{MR}}{\sqrt{d_M d_R}} \right)^\dagger - \frac{\{(f_{\alpha_L} \otimes I_{MR})^\dagger (f_{\tilde{\alpha}_L} \otimes I_{MR}), \bar{\rho}\}}{2d_M d_R} \right) \\ & + \epsilon^2 \sum_{\alpha_R, \tilde{\alpha}_R=1}^{d_R^2-1} \Gamma_{\alpha_R, \tilde{\alpha}_R}^{(R)} \left(\left(\frac{I_{LM}}{\sqrt{d_L d_M}} \otimes f_{\tilde{\alpha}_R} \right) \bar{\rho} \left(\frac{I_{LM}}{\sqrt{d_L d_M}} \otimes f_{\alpha_R} \right)^\dagger - \frac{\{(I_{LM} \otimes f_{\alpha_R})^\dagger (I_{LM} \otimes f_{\tilde{\alpha}_R}), \bar{\rho}\}}{2d_L d_M} \right), \end{aligned} \quad (23)$$

where $I_{MR} = I_M \otimes I_R$, $I_{LM} = I_L \otimes I_M$, where I_L and I_R are identity operators on the Hilbert spaces \mathcal{H}_L and \mathcal{H}_R [see Fig. 1]. Here d_L (d_R) is the dimension of the Hilbert space \mathcal{H}_L (\mathcal{H}_R). $d = d_L d_M d_R$ is the dimension of the total Hilbert space $\mathcal{H} = \mathcal{H}_L \otimes \mathcal{H}_M \otimes \mathcal{H}_R$, where d_M is the dimension of the Hilbert space \mathcal{H}_M . $\Gamma_{\alpha_L, \tilde{\alpha}_L}^{(L)}$, $\Gamma_{\alpha_R, \tilde{\alpha}_R}^{(R)}$ are positive-semidefinite matrices, $H_{LS}^{(L)}$, $H_{LS}^{(R)}$ are Hermitian and f_{α_L} , f_{α_R} are orthonormal basis of operators in the parts of the system connected to the left and right baths respectively, where orthonormality is defined

according to the Hilbert Schmidt inner product given by $\langle A | B \rangle = \text{Tr}(A^\dagger B)$. We choose the basis such that $f_{\alpha_L=d_L^2} = I_L / \sqrt{d_L}$, $f_{\alpha_R=d_R^2} = I_R / \sqrt{d_R}$.

3. Accurate populations and thermalization

Third, one might want the Markovian QME to recover the correct leading-order populations of the exact NESS

$$\bar{\rho}_{\text{NESS}}^{(0)} = \rho_{\text{NESS}}^{(0)} \quad (24)$$

The conditions for this have been described in Ref. 34 and are also explained as follows: Using the same argument as in Sec. II B, we can conclude that $\bar{\rho}_{\text{NESS}}^{(0)}$ is diagonal in energy eigenbasis [see Eq. (12)]. We start with writing down the RE for the given setup. and by solving Eq. (14), we get p_α in $\rho_{\text{NESS}}^{(0)}$ [Eq. (13)]. Then, in order to obtain the correct value of $\bar{\rho}_{\text{NESS}}^{(0)}$ as in Eq. (24), \mathcal{L}'_2 in Eq. (21) must satisfy the same Eq. (14) as \mathcal{L}_2 in RE [Eq. (18)]. Thus, we must have

$$\langle E_\alpha | \mathcal{L}'_2[\rho_{\text{NESS}}^{(0)}] | E_\alpha \rangle = \langle E_\alpha | \mathcal{L}_2[\rho_{\text{NESS}}^{(0)}] | E_\alpha \rangle = 0, \quad \forall \alpha. \quad (25)$$

In the equilibrium ($\beta_L = \beta_R = \beta$) scenario, Eq. (25) becomes the condition for thermalization [34]. Thermalization implies that after an infinite time, the steady state reaches the thermal state at a temperature defined by $\beta = 1/T$ when all the baths attached to the system are at temperature T , or in other words, we have $p_\alpha \propto e^{-\beta E_\alpha}$ in Eq. (25). The equilibrium case is just a special case of the non-equilibrium ($\beta_L \neq \beta_R$) scenario where one has to solve the linear equations obtained from RE to obtain p_α .

We remark that for physical consistency, it is necessary that one must preserve local conservation laws [Eq. (22)] and if the system is not driven and all baths have the same temperature (i.e. $\beta_L = \beta_R = \beta$), the system must thermalize to the common temperature of the baths. Both of these conditions are known to hold for RE as shown in Refs. 19 and 34.

4. Accurate populations and coherences

Finally, to recover the leading-order coherences of the exact NESS, i.e.

$$\langle E_\alpha | \bar{\rho}_{\text{NESS}}^{(2)} | E_\nu \rangle = \langle E_\alpha | \rho_{\text{NESS}}^{(2)} | E_\nu \rangle, \quad \forall \alpha \neq \nu \quad (26)$$

given that one has obtained $\bar{\rho}_{\text{NESS}}^{(0)} = \rho_{\text{NESS}}^{(0)}$, \mathcal{L}'_2 must yield exactly the same set of equations as Eq. (15). Therefore,

$$\langle E_\alpha | \mathcal{L}'_2[\rho_{\text{NESS}}^{(0)}] | E_\nu \rangle = \langle E_\alpha | \mathcal{L}_2[\rho_{\text{NESS}}^{(0)}] | E_\nu \rangle \quad \forall \alpha \neq \nu. \quad (27)$$

These [Secs. IID 1, IID 2, IID 3, IID 4] are the four steady-state requirements we have considered in this work.

E. CPTP and Local conservation laws with accurate populations

Let us investigate the conditions necessary for obtaining a Markovian QME in Lindblad form (or LE) [Sec. IID 1] that satisfies local conservation laws [Sec. IID 2] and yields accurate populations [Sec. IID 3].

To ensure local conservation laws hold and the QME is in Lindblad form, we ensure that our $\mathcal{L}'_2[\rho_{\text{NESS}}^{(0)}]$ is of the form given in Eq. (23). If one is additionally interested in checking if Eq. (25) is satisfied or not, one can simply check whether the following quantity τ^{pop} equals zero or not, where

$$\tau^{\text{pop}} = \sum_\alpha |\langle E_\alpha | \mathcal{L}'_2[\rho_{\text{NESS}}^{(0)}] | E_\alpha \rangle|. \quad (28)$$

τ^{pop} is a function of the fixed value of $\rho_{\text{NESS}}^{(0)}$, the exact QME, while the variable to be optimized over is \mathcal{L}'_2 consisting of $H_{LS}^{(i)}$, $\Gamma^{(i)}$, $i \in \{L, R\}$. Note that $\tau^{\text{pop}} = 0$ iff Eq. (25) holds, making it sufficient to work with τ^{pop} to see if Eq. (25) is satisfied. This can be formulated in the form of an optimization problem, in the same manner as done for the thermalization optimization problem (TOP) in Ref. 19. Here we consider the more general $\beta_L \neq \beta_R$ non-equilibrium case rather than the equilibrium scenario in the TOP, as given by varying H_{LS} , Γ for both left and right baths. We remind the reader that we only require to solve d equations in d variables to obtain p_α in Eq. (13) for this optimization problem in the non-equilibrium scenario.

$$\begin{aligned} \text{minimize : } & \tau^{\text{pop}} \text{ by varying } H_{LS}^{(L)}, H_{LS}^{(R)}, \Gamma^{(L)}, \Gamma^{(R)} \\ \text{subject to : } & H_{LS}^{(L)}, H_{LS}^{(R)} \text{ are hermitian,} \\ & \text{Tr}(\Gamma^{(L)}) = 1, \quad \Gamma^{(L)} \geq 0, \\ & \text{Tr}(\Gamma^{(R)}) = 1, \quad \Gamma^{(R)} \geq 0, \end{aligned} \quad (29)$$

Here $\Gamma^{(i)} \geq 0$ means $\Gamma^{(i)}$ is a positive semi-definite matrix. Note that the choice of $\text{Tr}(\Gamma^{(L)}) = \text{Tr}(\Gamma^{(R)}) = 1$ in Eq. (29) is completely arbitrary scaling, and can be set to other fixed values as well. In the optimization problem, let $\tau_{\text{opt}}^{\text{pop}}$ be the optimal value obtained from solving Eq. (29). Given a tolerance δ_{tol} ,

$$\text{if } \begin{cases} \tau_{\text{opt}}^{\text{pop}} < \delta_{\text{tol}}, & \text{the desired LE maybe possible,} \\ \tau_{\text{opt}}^{\text{pop}} \geq \delta_{\text{tol}} & \text{the desired LE is impossible,} \end{cases} \quad (30)$$

For $\tau_{\text{opt}}^{\text{pop}} > 0$, it will be interesting to know how far away the zeroth-order non-equilibrium steady state ($\bar{\rho}_{\text{NESS}}^{(0)}$) obtained via any LE satisfying local conservation laws [Eq. (23)] is from the exact zeroth-order NESS obtained from RE ($\rho_{\text{NESS}}^{(0)}$), as a way of understanding how “good” the leading-order NESS obtained from the LE is going to be. This can be calculated in the form of trace distance between the two density matrices, which we present in the form of a lemma.

Lemma 1. Let $\bar{\rho}_{\text{NESS}}^{(0)}$ be the zeroth-order NESS obtained via any LE satisfying local conservation laws [Eq. (23)], and $\rho_{\text{NESS}}^{(0)}$ as the exact zeroth-order NESS.

$$\text{Tracedist}(\bar{\rho}_{\text{NESS}}^{(0)}, \rho_{\text{NESS}}^{(0)}) \geq \frac{\tau_{\text{opt}}^{\text{pop}}}{2(t_L d_L^3 + t_R d_R^3 - t_L d_L - t_R d_R)} \quad (31)$$

where $\tau_{\text{opt}}^{\text{pop}}$ is the optimal value obtained from Eq. (29), d is the dimension of the Hilbert space of the system, while d_L (d_R) is the dimension of the Hilbert space of the part of the system connected to the left (right) bath [see Fig. 1].

Details of the proof of this Lemma is given in appendix B. This result highlights that for any non-zero $\tau_{\text{opt}}^{\text{pop}}$ value, the trace distance between the exact zeroth-order NESS and the NESS obtained from *any* LE satisfying local conservation laws has a non-zero lower bound of $\tau_{\text{opt}}^{\text{pop}}/\alpha$, where, from Eq. (31), $\alpha = 2(t_L(d_L^3 - d_L) + t_R(d_R^3 - d_R))$.

F. CPTP and Local conservation laws with accurate populations and coherences

Just as in the last subsection, if one is interested in checking whether both Eqs. (25) and (27) are satisfied or not (along with local conservation laws), then it is equivalent to checking whether $\mathcal{L}'_2[\rho_{\text{NESS}}^{(0)}]$ equals $\mathcal{L}_2[\rho_{\text{NESS}}^{(0)}]$. Note that $\mathcal{L}_2[\rho_{\text{NESS}}^{(0)}]$ is guaranteed to be zero along the diagonal by the construction of $\rho_{\text{NESS}}^{(0)}$. Thus, we can check whether $\tau^{\text{pop,coh}}$ equals zero or not, where $\tau^{\text{pop,coh}}$ is defined as

$$\tau^{\text{pop,coh}} = \left\| \mathcal{L}'_2[\rho_{\text{NESS}}^{(0)}] - \mathcal{L}_2[\rho_{\text{NESS}}^{(0)}] \right\|_2. \quad (32)$$

Eq. (32) highlights how far $\mathcal{L}'_2[\rho_{\text{NESS}}^{(0)}]$ is from $\mathcal{L}_2[\rho_{\text{NESS}}^{(0)}]$, in the form of the 2-norm function, although this choice of norm is arbitrary and any p -norm ($\|\cdots\|_p$) can be used (fundamentally, we only require that the resulting optimization problem be an SDP). When $\mathcal{L}'_2[\rho_{\text{NESS}}^{(0)}] = \mathcal{L}_2[\rho_{\text{NESS}}^{(0)}]$, $\tau^{\text{pop,coh}} = 0$, and we have a LE whose NESS recovers correct populations and coherences while satisfying local conservation laws. This can again be formulated as an optimization problem given by

$$\begin{aligned} & \text{minimize : } \tau^{\text{pop,coh}} \text{ by varying } H_{LS}^{(L)}, H_{LS}^{(R)}, \Gamma^{(L)}, \Gamma^{(R)} \\ & \text{subject to : } H_{LS}^{(L)}, H_{LS}^{(R)} \text{ are hermitian,} \\ & \quad \text{Tr}(\Gamma^{(L)}) = 1, \quad \Gamma^{(L)} \geq 0, \\ & \quad \text{Tr}(\Gamma^{(R)}) = 1, \quad \Gamma^{(R)} \geq 0, \end{aligned} \quad (33)$$

Given that $\text{Tr}(\Gamma^{(i)}) = t_i$, $i \in \{L, R\}$, then

Similarly as in Sec. II E, let $\tau_{\text{opt}}^{\text{pop,coh}}$ be the optimal value obtained from solving Eq. (33). With the same tolerance δ_{tol} :

$$\text{if } \begin{cases} \tau_{\text{opt}}^{\text{pop,coh}} < \delta_{\text{tol}}, & \text{desired LE maybe possible,} \\ \tau_{\text{opt}}^{\text{pop,coh}} \geq \delta_{\text{tol}} & \text{desired LE is impossible,} \end{cases} \quad (34)$$

Notice that both Eqs. (29) and (33) are SDPs, and are similar to the TOP problem in Ref. 19. Therefore, they can be directly put into standard packages for disciplined convex optimization like the CVX MATLAB [43] package which automatically outputs the correct optimal value and gives one set of optimal values for $H_{LS}^{(L)}$, $H_{LS}^{(R)}$, $\Gamma^{(L)}$ and $\Gamma^{(R)}$. Thus, if $\tau_{\text{opt}}^{\text{pop}}, \tau_{\text{opt}}^{\text{pop,coh}} < \delta_{\text{tol}}$, it not only says that the desired type of LE may be possible but it also outputs one possible candidate for such a LE. If $\tau_{\text{opt}}^{\text{pop}}, \tau_{\text{opt}}^{\text{pop,coh}} \geq \delta_{\text{tol}}$, the desired type of LE is impossible. Notice that satisfying $\tau_{\text{opt}}^{\text{pop,coh}} \leq \delta_{\text{tol}}$ implies that getting correct coherences of second-order NESS and correct populations of zeroth-order NESS may be possible via an LE, but $\tau_{\text{opt}}^{\text{pop,coh}} > \delta_{\text{tol}}$ implies that either the LE NESS fails to capture the correct leading-order populations of the exact NESS and/or the correct leading-order coherences of the exact NESS. In other words, for $\tau_{\text{opt}}^{\text{pop,coh}} > \delta_{\text{tol}}$, there exists no LE whose NESS gets the correct leading-order populations and coherences.

We again remark that in all of the above, p_α [Eq. (13)] can be easily obtained by solving the RE. Moreover, one only has to solve d equations in d variables to obtain p_α from RE. This task is much easier than solving the RE itself. Also note here that checking if LE obtains accurate leading-order coherences separately from accurate leading-order populations [Eq. (15) with $\bar{\rho}_{\text{NESS}}^{(0)}$ instead of $\rho_{\text{NESS}}^{(0)}$ in the second term] is not an SDP. This is because we require $\bar{\rho}_{\text{NESS}}^{(0)}$ to be computed before that, which means \mathcal{L}'_2 and $\bar{\rho}_{\text{NESS}}^{(0)}$ are both variables in this case only satisfying Eq. (14) (here $\bar{\rho}_{\text{NESS}}^{(0)}$ in general need not be equal to $\rho_{\text{NESS}}^{(0)}$).

III. DISCUSSION OF NUMERICAL RESULTS

We will now use the formulated optimization problems to analyze a specific system-bath setup. By implementing our semidefinite programming framework, we aim to

$N_L = N_R$	$\tau_{\text{opt}}^{\text{pop}} \text{ v/s } \beta$	$\tau_{\text{opt}}^{\text{pop,coh}} \text{ v/s } \beta$	$\tau_{\text{opt}}^{\text{pop}} \text{ v/s } g$	$\tau_{\text{opt}}^{\text{pop,coh}} \text{ v/s } g$	Correct populations	Correct coherences
1	Fig. 2(a)	Fig. 2(b)	Fig. 2(c)	Fig. 2(d)	Impossible	Impossible
2	Fig. 3(a)	Fig. 3(b)	Fig. 3(c)	Fig. 3(d)	Maybe possible	Impossible

TABLE I. Table of figure references summarising our results in the non-equilibrium ($\beta_L \neq \beta_R$) scenario for different energy biases and number of qubits N_L, N_R attached to the left and right baths respectively. All plots are done for system-bath coupling $\epsilon = 0.01$. The columns for ‘‘Correct populations’’ and ‘‘Correct coherences’’ highlight the possibilities for obtaining correct leading-order diagonal and off-diagonal terms respectively in the steady state in a wide parameter regime. In very special scenarios that is equilibrium and very low inter-site coupling g , it might be feasible to get correct populations and/or correct coherences.

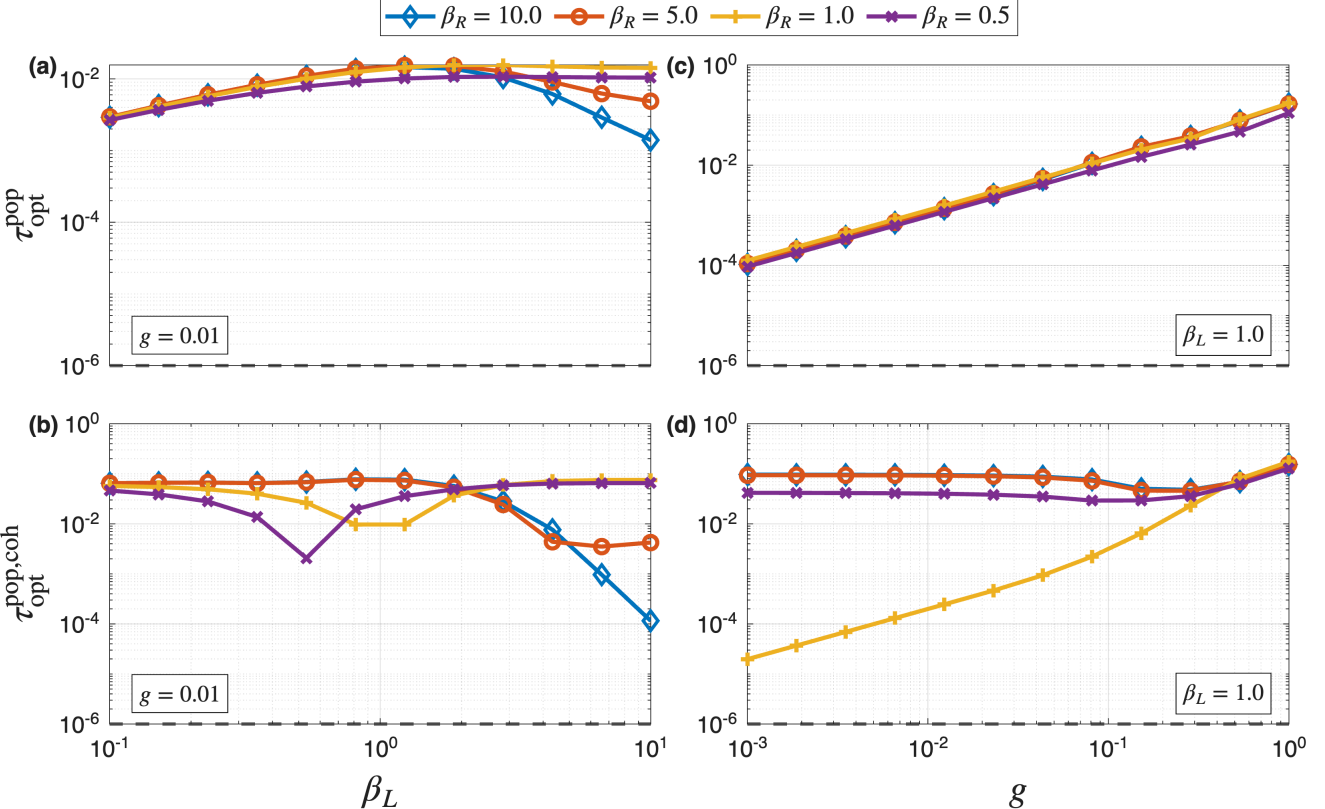


FIG. 2. Plots for $N_L = N_R = 1$, $N_M = 2$ for the isotropic XXZ Hamiltonian [Eq. (35)] keeping $\gamma_\ell = 1 \forall \ell$, $\omega_c = 10$ [Eq. (42)] and $\beta_R = 10.0$ (blue diamond), 5.0 (orange circle), 1.0 (yellow plus), 0.5 (purple cross). The black dashed horizontal line represents the chosen tolerance $\delta_{\text{tol}} = 10^{-6}$. (a) $\tau_{\text{opt}}^{\text{pop}}$ [Eq. (29)] versus β_L with $g = 0.01$. (b) $\tau_{\text{opt}}^{\text{pop,coh}}$ [Eq. (33)] versus β_L with $g = 0.01$. (c) $\tau_{\text{opt}}^{\text{pop}}$ versus g for $\beta_L = 1.0$. (d) $\tau_{\text{opt}}^{\text{pop,coh}}$ versus g for $\beta_L = 1.0$. This figure shows that it is impossible to achieve populations correctly up to leading-order (implying incorrect coherences as well) for only single qubits attached to left and right baths as discussed in Sec. III A.

determine whether a physically consistent LE can be constructed for this setup while satisfying the desired properties laid down in Sec. IID. This analysis will provide insights into the feasibility of different dynamical behaviors and potentially reveal fundamental limitations on the existence of such LEs.

In particular, we study the possibility of having a Lindblad description satisfying local conservation laws [Sec. IID 2] and obtaining correct populations [Secs. IID 3, IIE] and coherences [Secs. IID 4, IIF] of the zeroth-order and second-order, for non-equilibrium (or equilibrium with $\beta_L = \beta_R$) steady states in open isotropic

XXZ qubit chain system with some of the qubits attached to baths modelled by an infinite number of bosonic modes. We will start by describing our setup.

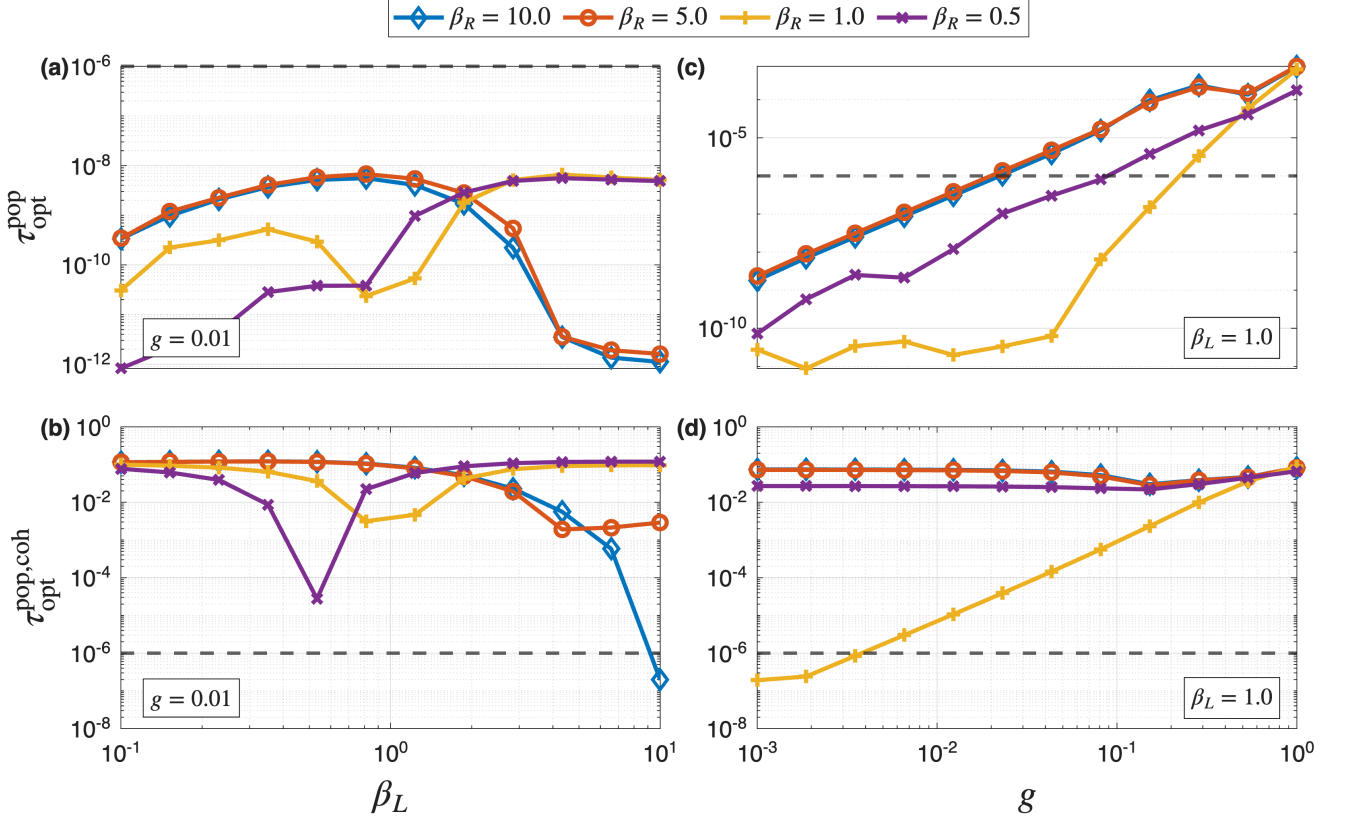


FIG. 3. Plots for $N_L = N_R = 2$, $N_M = 2$ (i.e. two qubits attached to left and right baths, see Sec. III B) for the isotropic XXZ Hamiltonian [Eq. (35)] keeping $\gamma_\ell = 1 \forall \ell$, $\omega_c = 10$ [Eq. (42)] and $\beta_R = 10.0$ (blue diamond), 5.0 (red circle), 1.0 (yellow cross), 0.5 (purple plus). The black dashed horizontal line represents $\delta_{\text{tol}} = 10^{-6}$. (a) $\tau_{\text{opt}}^{\text{pop}}$ [Eq. (29)] versus β_L with $g = 0.01$. (b) $\tau_{\text{opt}}^{\text{pop,coh}}$ [Eq. (33)] versus β_L with $g = 0.01$. (c) $\tau_{\text{opt}}^{\text{pop}}$ versus g for $\beta_L = 1.0$. (d) $\tau_{\text{opt}}^{\text{pop,coh}}$ versus g for $\beta_L = 1.0$. This figure shows that it might be possible to obtain steady-states with correct leading-order populations for low inter-site coupling, but it is impossible to obtain both correct leading-order populations and coherences generally.

The Hamiltonian for this setup is given by

$$\begin{aligned}
 H &= H_S + H_{SB} + H_B, \\
 H_S &= \omega_0 \sum_{\ell=1}^N \sigma_z^{(\ell)} + g \sum_{\ell=1}^{N-1} (\sigma_x^{(\ell)} \sigma_x^{(\ell+1)} + \sigma_y^{(\ell)} \sigma_y^{(\ell+1)} \\
 &\quad + \sigma_z^{(\ell)} \sigma_z^{(\ell+1)}), \\
 H_{SB} &= \sum_{\ell \in \{N_L, N_R\}} \sum_{r=1}^{\infty} (\kappa_{\ell r} B_r^{(\ell)\dagger} \sigma_-^{(\ell)} + \kappa_{\ell r}^* B_r^{(\ell)} \sigma_+^{(\ell)}), \\
 H_B &= \sum_{\ell \in \{N_L, N_R\}} \sum_{r=1}^{\infty} \Omega_r^\ell B_r^{(\ell)\dagger} B_r^{(\ell)},
 \end{aligned} \tag{35}$$

where $\sigma_{x,y,z}^{(\ell)}$ denotes the Pauli matrices acting on the ℓ^{th} qubit, $\sigma_+^{(\ell)} = (\sigma_x^{(\ell)} + i\sigma_y^{(\ell)})/2$, $\sigma_-^{(\ell)} = (\sigma_x^{(\ell)} - i\sigma_y^{(\ell)})/2$, $B_r^{(\ell)}$ is bosonic annihilation operator for the r^{th} mode of the bath attached at the ℓ^{th} site. Here $\omega_0^{(\ell)}$ and g represent the magnetic field and the overall qubit-qubit coupling strength. The first N_L and the last N_R qubits are attached to the left and right baths, while the remaining $N_M = N - N_L - N_R$ qubits are not attached to any bath.

The specific setup falls under the schematic structure of Fig. 1.

At initial time, the baths are taken to be in their respective thermal state with inverse temperatures β_ℓ and chemical potentials μ_ℓ . The dynamics of the system can be shown to be governed by the bath spectral functions, defined as

$$\mathfrak{J}_\ell(\omega) = 2\pi \sum_{k=0}^{\infty} |\kappa_{\ell k}|^2 \delta(\omega - \Omega_k^\ell) \tag{36}$$

and the Bose distribution,

$$n_\ell(\omega) = [e^{\beta_\ell \omega} - 1]^{-1}, \tag{37}$$

corresponding to the initial states of the baths. The RE for this set-up is obtained by simplification of Eq. (19), which gives the following.

$$\begin{aligned}
 \frac{\partial \rho}{\partial t} &= i[\rho, H_S] \\
 &\quad - \epsilon^2 \sum_{\ell} \left([S_\ell^\dagger, S_\ell^{(1)} \rho] + [\rho S_\ell^{(2)}, S_\ell^\dagger] + \text{H.c.} \right),
 \end{aligned} \tag{38}$$

where S_ℓ is the system operator at ℓ th site coupling with the corresponding bath and

$$\begin{aligned} S_\ell^{(1)} &= \int_0^\infty dt' \int \frac{d\omega}{2\pi} S_\ell(-t') e^{\beta_\ell(\omega - \mu_\ell)} \mathfrak{J}_\ell(\omega) n_\ell(\omega) e^{-i\omega t'}, \\ S_\ell^{(2)} &= \int_0^\infty dt' \int \frac{d\omega}{2\pi} S_\ell(-t') \mathfrak{J}_\ell(\omega) n_\ell(\omega) e^{-i\omega t'}, \end{aligned} \quad (39)$$

with $S_\ell(t) = e^{iH_{St}} S_\ell e^{-iH_{St}}$, and H.c. denoting Hermitian conjugate. For our setting, we have $S_\ell = \sigma_-^{(\ell)}$. Putting this in Eq. (38), we note that the second-order dissipator (\mathcal{L}_2) of the RE is [34]

$$\begin{aligned} \mathcal{L}_2(\rho) = \sum_\ell \sum_{\alpha, \gamma=1}^{2^N} & \{ [\rho |E_\alpha\rangle \langle E_\alpha| \sigma_-^{(\ell)} |E_\gamma\rangle \langle E_\gamma|, \sigma_+^{(\ell)}] C_\ell(\alpha, \gamma) \\ & + [\sigma_+^{(\ell)}, |E_\alpha\rangle \langle E_\alpha| \sigma_-^{(\ell)} |E_\gamma\rangle \langle E_\gamma|] D_\ell(\alpha, \gamma) + \text{H.c.}\}, \end{aligned} \quad (40)$$

with

$$\begin{aligned} C_\ell(\alpha, \gamma) &= \frac{\mathfrak{J}_\ell(E_{\gamma\alpha}) n_\ell(E_{\gamma\alpha})}{2} - i\mathcal{P} \int_0^\infty d\omega \frac{\mathfrak{J}_\ell(\omega) n_\ell(\omega)}{\omega - E_{\gamma\alpha}}, \\ D_\ell(\alpha, \gamma) &= \frac{e^{\beta_\ell(E_{\gamma\alpha} - \mu_\ell)} \mathfrak{J}_\ell(E_{\gamma\alpha}) n_\ell(E_{\gamma\alpha})}{2} \\ & - i\mathcal{P} \int_0^\infty d\omega \frac{e^{\beta_\ell(\omega - \mu_\ell)} \mathfrak{J}_\ell(\omega) n_\ell(\omega)}{\omega - E_{\gamma\alpha}}, \end{aligned} \quad (41)$$

where \mathcal{P} denotes the Cauchy Principal value, and $E_{\gamma\alpha} = E_\gamma - E_\alpha$. We consider bosonic baths described by Ohmic spectral functions with Gaussian cut-offs,

$$\mathfrak{J}_\ell(\omega) = \gamma_\ell \omega e^{-(\omega/\omega_c)^2} \Theta(\omega), \quad (42)$$

where, $\Theta(\omega)$ is Heaviside step function, γ_ℓ is the coupling strength between ℓ^{th} qubit and bath and ω_c is the cut-off frequency (set to $\omega_c = 10$ for all figures in this work).

We are interested in finding a Markovian description that accurately captures the steady-state density matrix in the above setting. As mentioned before in Sec. II C, the RE is known to give accurate populations and coherences to leading-order in system-bath coupling, as well as, respect all local conservation laws. In the above setting, it also captures thermalization of the isotropic XXZ-chain when all baths are at the same temperature. However, the RE can also be shown to not respect the CPTP property, and can lead to density matrix having negative eigenvalues of small magnitude. The question then is, whether there exists any physically consistent Markovian description, i.e., an LE which respects local conservation laws, gives correct populations and coherences to leading-order in system-bath coupling, and has CPTP property by definition. We use our SDP based formalism developed in Sec. II D to answer this question.

In particular, we get $\tau_{\text{opt}}^{\text{pop}}$ [Eq. (29)] for understanding whether any LE can get correct populations of $\rho_{\text{NESS}}^{(0)}$, or get $\tau_{\text{opt}}^{\text{pop,coh}}$ [Eq. (29)] for understanding whether the

LE can get both correct populations and coherences of $\rho_{\text{NESS}}^{(2)}$. We construct the basis for operators in Hilbert space of the first N_L and last N_R qubits, so that the most general form of the desired LE can be written as in Eq. (23). For the ℓ th qubit, we choose the orthonormal basis $\{-\sigma_z^{(\ell)}/\sqrt{2}, \sigma_+^{(\ell)}, \sigma_-^{(\ell)}, I_2^{(\ell)}/\sqrt{2}\}$, and $I_2^{(\ell)}$ is the identity operator for the qubit Hilbert space. The basis for the first N_L and the last N_R qubits is obtained by direct product of the basis of each of the qubits. The optimization problems are set in this basis, which we then directly input in the CVX MATLAB package to obtain $\tau_{\text{opt}}^{\text{pop}}$, $\tau_{\text{opt}}^{\text{pop,coh}}$. We set a value of the tolerance $\delta_{\text{tol}} = 10^{-6}$, as in Ref. 19.

A. Single qubit attached to left and right baths

First, we consider the case where the first and last qubit of the chain are coupled to the left and right baths, respectively, which means $N_L = N_R = 1$. We analyze the behavior of $\tau_{\text{opt}}^{\text{pop}}$ and $\tau_{\text{opt}}^{\text{pop,coh}}$ under different conditions using the isotropic XXZ Hamiltonian with $N_M = 2$, while keeping $\beta_L = 1.0$. The findings are summarized below.

Our analysis first considers the effect of varying the inter-qubit coupling strength g for several values of β_R , as depicted in Figs. 2(c,d) and A1(c,d). The results for the $N_L = N_R = 1$ case consistently show that $\tau_{\text{opt}}^{\text{pop}}$ and $\tau_{\text{opt}}^{\text{pop,coh}}$ are significantly greater than the tolerance δ_{tol} . This finding explicitly rules out the possibility of a general LE that can simultaneously preserve complete positivity, obey local conservation laws, and correctly capture the leading-order populations or coherences within this parameter range. We observe that both $\tau_{\text{opt}}^{\text{pop}}$ and $\tau_{\text{opt}}^{\text{pop,coh}}$ increase with g , which generally aligns with previous results [34, 44] suggesting that local Lindblad equations provide a better description only when the system-qubit coupling is weak. The accurate capture of these coherences is critical, as they play a significant role in quantum thermodynamic processes [30, 45].

In contrast, the analysis of varying β_L while keeping a fixed $g = 0.01$ reveals the same behaviour of populations and coherences being above the tolerance δ_{tol} , as shown in Figs. 2(a,b) and A1(a,b). At both non-equilibrium and equilibrium, the values of $\tau_{\text{opt}}^{\text{pop}}$ and $\tau_{\text{opt}}^{\text{pop,coh}}$ are much larger than δ_{tol} . The conclusion is that constructing a fully consistent LE with only a single qubit coupled to baths at the left and right sites is not possible over a very large parameter regime.

B. Two qubits attached to left and right baths

We consider the case where the first and last two qubits of the chain are coupled to the left and right baths, respectively, which means $N_L = N_R = 2$. We analyze

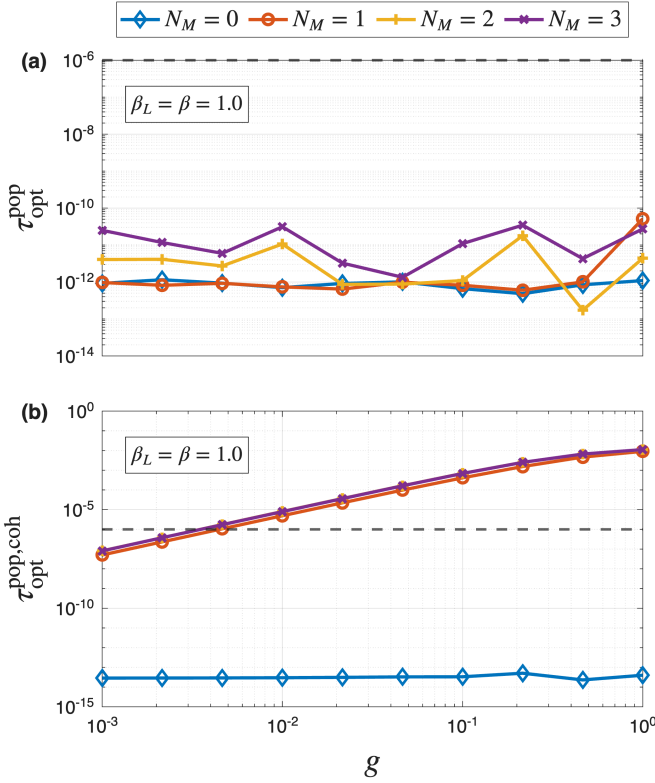


FIG. 4. Plots for (a) $\tau_{\text{opt}}^{\text{pop}}$ [Eq. (29)] and (b) $\tau_{\text{opt}}^{\text{pop,coh}}$ [Eq. (33)] versus g with $N_L = 3$, $N_R = 0$, $\beta_L = \beta = 1.0$ for isotropic XXZ Hamiltonian and four different values of $N_M = 0$ (blue diamond), 1 (red circle), 2 (yellow cross), 3 (purple plus). The black dashed curve denotes $\delta_{\text{tol}} = 10^{-6}$ with $\gamma_\ell = 1 \forall \ell$, $\omega_c = 10$ [Eq. (42)].

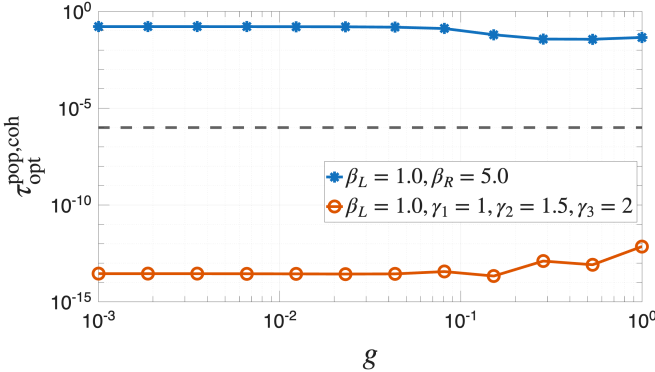


FIG. 5. Plots for $\tau_{\text{opt}}^{\text{pop,coh}}$ [Eq. (33)] with $N_L = 3$, $N_M = N_R = 0$ with $\beta_L = \beta = 1.0$, $\gamma_1 = 1$, $\gamma_2 = 1.5$, $\gamma_3 = 2$ (red circle) and $N_L = 1$, $N_M = 0$, $N_R = 2$ with $\beta_L = 1.0$, $\beta_R = 5.0$, $\gamma_\ell = 1 \forall \ell$ (blue star) versus g . The black dashed curve denotes $\delta_{\text{tol}} = 10^{-6}$ and $\omega_c = 10$ [Eq. (42)].

the behavior of $\tau_{\text{opt}}^{\text{pop}}$ and $\tau_{\text{opt}}^{\text{pop,coh}}$ under different conditions using the same parameters as in Sec. III A. We note that local two-qubit Lindbladian dissipators have previously been employed to study energy transport in similar spin chains [46–48]. Our findings are summarized below.

Our results plotted in Figs. 3 and A2. We find a significant departure from the previous case in Sec. III A as $\tau_{\text{opt}}^{\text{pop}} \ll \delta_{\text{tol}}$ for a relatively wider range of $g < 0.1$, as shown in Figs. 3(c,d). This range increases as β_L approaches β_R (i.e. equilibrium). This suggests that, unlike the $N_L = N_R = 1$ case, a LE that preserves complete positivity, obeys local conservation laws, and correctly captures zeroth-order populations may be possible even for non-equilibrium steady states. Despite the viability for populations, we find that $\tau_{\text{opt}}^{\text{pop,coh}} \gg \delta_{\text{tol}}$ across most parameters, except at equilibrium or for very low g values, indicating that coherences and populations *together* remain difficult to capture.

Upon varying β_L while keeping $g = 0.01$ (Figs. 3(a,b) and A2(a,b)), non-monotonic trends in $\tau_{\text{opt}}^{\text{pop}}$, $\tau_{\text{opt}}^{\text{pop,coh}}$ are observed. We find $\tau_{\text{opt}}^{\text{pop}} \ll \delta_{\text{tol}}$ across a wide range of β_L . It is observed that $\tau_{\text{opt}}^{\text{pop,coh}} \gg \delta_{\text{tol}}$, except at equilibrium. This is consistent with previous observations, given the weak coupling strength.

C. Correct populations and coherences with baths attached to all qubits

Here, we try a different setup from previous two subsections. First we keep $N_R = 0$ and attach Redfield baths of same temperature with the same coupling strength $\gamma_\ell = 1 \forall \ell$ [Eq. (42)] to each of the first N_L qubits. In this setup, when $N_M = 0$, it is seen that all of our desired physical properties are satisfied for the equilibrium (all baths of same temperature) scenario.

Fig. 4 highlights the results of this optimization by plotting $\tau_{\text{opt}}^{\text{pop}}$ (upper panel) and $\tau_{\text{opt}}^{\text{pop,coh}}$ (lower panel) versus different values of g . Most interestingly, we notice that when all the qubits of the system are connected to baths, it might be possible for the CVX-optimized Lindbladian baths to get the correct populations and coherences for its steady state, as $\tau_{\text{opt}}^{\text{pop,coh}} \ll \delta_{\text{tol}}$. We remark that we get similar results when we plot $\tau_{\text{opt}}^{\text{pop,coh}}$, $\tau_{\text{opt}}^{\text{pop}}$ versus $\beta_L = \beta$ for fixed $g = 0.01$ and the other parameters being the same.

For the case of $N_M = N_R = 0$ in Fig. 4, one might consider the equilibrium setup with all coupling strengths same to be a very special scenario, and wish to see how robust the equilibrium case is when the bath coupling strengths are different across the qubits. One might also question what happens in the non-equilibrium case of all sites attached to baths (i.e. when $N_M = 0$, $N_R \neq 0$ and $\beta_L \neq \beta_R$). Fig. 5 highlights these plots, showing that while the equilibrium case still gets all the desired physical properties even with different coupling strengths of the baths to the qubits, in the non-equilibrium scenario we again are unable to satisfy correct populations and coherences together.

IV. CONCLUSIONS AND OUTLOOK

The results presented in this work demonstrate the power of convex optimization, specifically semidefinite programming, in probing the physical consistency of quantum master equations. Our analysis reveals a range of parameter regimes, particularly in the presence of strong asymmetry in bath temperatures ($\beta_L \neq \beta_R$) or large inter-site couplings where no LE can simultaneously satisfy complete positivity, preserve local conservation laws, and yield the correct NESS populations and coherences (up to leading-order, see Table II). While we focused on these quantities in this study, we expect that other properties may be investigated in a similar manner, as long as they can be expressed as a suitable optimization problem. Moreover, albeit we focused on the isotropic XXZ qubit chain, our approach is readily adaptable to other Hamiltonian setups.

One of the central insights from our approach is the identification of the trade-offs between obtaining correct populations and coherences (up to leading-order), and the enforcement of conservation laws in Markovian models. While equilibrium configurations with low coupling strength showed marginal feasibility, the non-equilibrium setups failed to admit consistent Lindblad descriptions, validating earlier theoretical predictions [19].

Looking forward, this semidefinite programming (SDP) - based approach can be extended in various directions by formulating other desired properties, or combinations thereof, within the framework of SDPs. Importantly, such an SDP formulation provides not only candidate optimal solutions but also reliable and tight optimal values, via the associated dual problem. This yields rigorous and quantitatively reliable bounds on how closely the desired properties can be satisfied. An especially important regime is when the solution of the SDP certifies that the desired properties cannot be simultaneously satisfied, even approximately, thereby yielding rigorous no-go statements rather than merely constructive approximations. Moreover, these guarantees can be accessed in practice without explicitly constructing dual problems or establishing duality results by hand: modern SDP solvers implement primal-dual algorithms internally and automatically return optimal values. As a result, much of the analytical burden can be outsourced to well-developed numerical tools, allowing the focus to remain on formulating physically meaningful metrics and constraints.

Moreover, the emergence of quantum hardware for Noisy Intermediate Scale Quantum (NISQ) simulations offers an exciting avenue to validate these predictions experimentally, particularly in platforms capable of engineered dissipation such as trapped ions [49], Rydberg atoms [50], superconducting circuits [51], and semiconductor quantum dots [52], by comparing engineered Lindbladian dynamics to exact Redfield or microscopic evolution. Thus, our results present an interesting application of SDPs towards understanding open quantum system

dynamics and lay the foundation for future explorations into controlled dissipative quantum engineering.

All code used in this work can be found in Ref. 53.

V. ACKNOWLEDGEMENTS

We thank A. Dhar for useful discussions about this project. SS thanks the International Centre for Theoretical Sciences for its hospitality and acknowledges support via the Long Term Visiting Student Program (LTVSP). MK acknowledges the support of the Department of Atomic Energy, Government of India, under Project No. RTI4001. MK thanks the hospitality of the Department of Physics, Princeton University. Part of this work was performed at the Institute for Quantum Computing, at the University of Waterloo, which is supported by Innovation, Science, and Economic Development Canada. DT is supported by the Mike and Ophelia Lazaridis Fellowship. AP thanks IIT Hyderabad Seed Grant for support.

Appendix A: Calculation of $\rho_{\text{NESS}}^{(0)}$ from Redfield Equation

In this appendix, we derive the precise form of

$$\rho_{\text{NESS}}^{(0)} = \sum_{a=1}^d p_a |E_a\rangle \langle E_a|. \quad (\text{A1})$$

Here $d = 2^N$ is the dimension of our total system. We use the vector $\mathbf{p} = (p_1, p_2, \dots, p_\alpha \dots)^T$ and note that the second-order dissipator (\mathcal{L}_2) of the RE is [34]

$$\begin{aligned} \mathcal{L}_2(\rho) = & \sum_{\ell} \sum_{\alpha, \gamma=1}^{2^N} \{ [\rho |E_\alpha\rangle \langle E_\alpha| \sigma_-^{(\ell)} |E_\gamma\rangle \langle E_\gamma|, \sigma_+^{(\ell)}] C_\ell(\alpha, \gamma) \\ & + [\sigma_+^{(\ell)}, |E_\alpha\rangle \langle E_\alpha| \sigma_-^{(\ell)} |E_\gamma\rangle \langle E_\gamma|] D_\ell(\alpha, \gamma) + \text{H.c.}\}, \end{aligned} \quad (\text{A2})$$

with

$$\begin{aligned} C_\ell(\alpha, \gamma) &= \frac{\mathfrak{J}_\ell(E_{\gamma\alpha}) n_\ell(E_{\gamma\alpha})}{2} - i\mathcal{P} \int_0^\infty d\omega \frac{\mathfrak{J}_\ell(\omega) n_\ell(\omega)}{\omega - E_{\gamma\alpha}}, \\ D_\ell(\alpha, \gamma) &= \frac{e^{\beta_\ell(E_{\gamma\alpha} - \mu_\ell)} \mathfrak{J}_\ell(E_{\gamma\alpha}) n_\ell(E_{\gamma\alpha})}{2} \\ & - i\mathcal{P} \int_0^\infty d\omega \frac{e^{\beta_\ell(\omega - \mu_\ell)} \mathfrak{J}_\ell(\omega) n_\ell(\omega)}{\omega - E_{\gamma\alpha}}, \end{aligned} \quad (\text{A3})$$

where \mathcal{P} denotes the Cauchy Principal value, $E_{\gamma\alpha} = E_\gamma - E_\alpha$, $n_\ell(\omega) = (e^{\beta_\ell(\omega - \mu_\ell)} - 1)^{-1}$ is the average occupation number and $\mathfrak{J}_\ell(\omega)$ is the spectral bath function. We take an ohmic form $\mathfrak{J}_\ell(\omega) = \omega \exp(-(\omega/\omega_c)^2)$ for the spectral bath function. The summation over ℓ in Eq. (A2) is performed over the qubits where the

baths are connected ($\ell = 1, N$ for $N_L = N_R = 1$ and $\ell = 1, 2, N-1, N$ for $N_L = N_R = 2$) and $H_S |E_\alpha\rangle = E_\alpha |E_\alpha\rangle$. Now, from Eq. (14) of the main text, we know

that $\langle E_k | \mathcal{L}_2[\rho_{\text{NESS}}^{(0)}] | E_k \rangle = 0 \ \forall k$. We thus have

$$\begin{aligned} \langle E_k | \rho_{\text{NESS}}^{(0)} | E_k \rangle &= \sum_{\alpha, \gamma=1}^{2^N} \sum_{\ell} \{ p_\alpha \langle E_k | [|E_\alpha\rangle \langle E_\alpha | \sigma_-^{(\ell)} |E_\gamma\rangle \langle E_\gamma |, \sigma_+^{(\ell)}] | E_k \rangle C_\ell(\alpha, \gamma) \\ &+ p_\gamma \langle E_k | [\sigma_+^{(\ell)}, |E_\alpha\rangle \langle E_\alpha | \sigma_-^{(\ell)} |E_\gamma\rangle \langle E_\gamma |] | E_k \rangle D_\ell(\alpha, \gamma) + \text{H.c.} \}. \end{aligned} \quad (\text{A4})$$

In Eq. (A4), the L.H.S is 0, and the R.H.S can be written as a vector dot product. More precisely, we can rewrite Eq. (A4) as some matrix A multiplied with vector

\mathbf{p} giving the $\mathbf{0}$ vector ($A\mathbf{p} = \mathbf{0}$). The matrix elements A_{km} is given by collecting the coefficients of p_m in the R.H.S of Eq. (A4), giving us

$$\begin{aligned} A_{km} &= \sum_{\gamma=1}^{2^N} \sum_{\ell} \{ (\langle E_k | [|E_m\rangle \langle E_m | \sigma_-^{(\ell)} |E_\gamma\rangle \langle E_\gamma |, \sigma_+^{(\ell)}] | E_k \rangle C_\ell(m, \gamma) + \text{H.c.}) \\ &+ (\langle E_k | [\sigma_+^{(\ell)}, |E_\gamma\rangle \langle E_\gamma | \sigma_-^{(\ell)} |E_m\rangle \langle E_m |] | E_k \rangle D_\ell(\gamma, m) + \text{H.c.}) \}. \end{aligned} \quad (\text{A5})$$

Along with the constraints arising from p_a being the elements of a diagonal density matrix ($\sum_a p_a = 1, 0 \leq p_a \leq 1$), we can solve the equation $A\mathbf{p} = \mathbf{0}$ using standard linear equation solving techniques and arrive at \mathbf{p} . This gives us the required diagonal elements of $\rho_{\text{NESS}}^{(0)}$, presented in Eq. (A1).

Appendix B: Trace distance between the obtained and the exact zeroth-order steady state

In this section, we prove lemma 1 of the main text. First, we recall Eq. (29)

$$\tau^{\text{pop}} = \sum_{\alpha} |\langle E_\alpha | \mathcal{L}_2[\rho_{\text{NESS}}^{(0)}] | E_\alpha \rangle|, \quad (\text{B1})$$

and recall Lemma 1.

Lemma 1. Let $\bar{\rho}_{\text{NESS}}^{(0)}$ be the zeroth-order NESS obtained via any LÉ satisfying local conservation laws [Eq. (23)], and $\rho_{\text{NESS}}^{(0)}$ as the exact zeroth-order NESS. Given that $\text{Tr}(\Gamma^{(i)}) = t_i, i \in \{L, R\}$, then

$$\text{Tracedist}(\bar{\rho}_{\text{NESS}}^{(0)}, \rho_{\text{NESS}}^{(0)}) \geq \frac{\tau_{\text{opt}}^{\text{pop}}}{2(t_L d_L^3 + t_R d_R^3 - t_L d_L - t_R d_R)} \quad (31)$$

where $\tau_{\text{opt}}^{\text{pop}}$ is the optimal value obtained from Eq. (29), d is the dimension of the Hilbert space of the system, while d_L (d_R) is the dimension of the Hilbert space of the part of the system connected to the left (right) bath [see Fig. 1].

Proof. Recall from Eq. (A1) that $\rho_{\text{NESS}}^{(0)} = \sum_a p_a |E_a\rangle \langle E_a|$ is the non-equilibrium steady state

obtained from RE with second-order dissipator \mathcal{L}_2 as per Appendix A [Eq. (A2)]. Here, recall that $\{|E_a\rangle\}$ is the energy eigenbasis of our system Hamiltonian H_S . On the other hand, $\bar{\rho}_{\text{NESS}}^{(0)} = \sum_a p'_a |E_a\rangle \langle E_a|$ is the zeroth-order steady state of the master equation with the general Lindbladian second-order dissipator \mathcal{L}'_2 as

$N_L = N_R$	$\tau_{\text{opt}}^{\text{pop}}$ v/s β	$\tau_{\text{opt}}^{\text{pop,coh}}$ v/s β	$\tau_{\text{opt}}^{\text{pop}}$ v/s g	$\tau_{\text{opt}}^{\text{pop,coh}}$ v/s g	Correct populations	Correct coherences
1	Fig. A1(a)	Fig. A1(b)	Fig. A1(c)	Fig. A1(d)	Impossible	Impossible
2	Fig. A2(a)	Fig. A2(b)	Fig. A2(c)	Fig. A2(d)	Maybe possible	Impossible

TABLE II. Table of figure references summarising our results in the non-equilibrium ($\beta_L \neq \beta_R$) scenario for different energy biases and number of qubits N_L, N_R attached to the left and right baths respectively in the biased case of $\epsilon_0 = 0.01$ [Sec. C]. All plots are done for system-bath coupling $\epsilon = 0.01$.

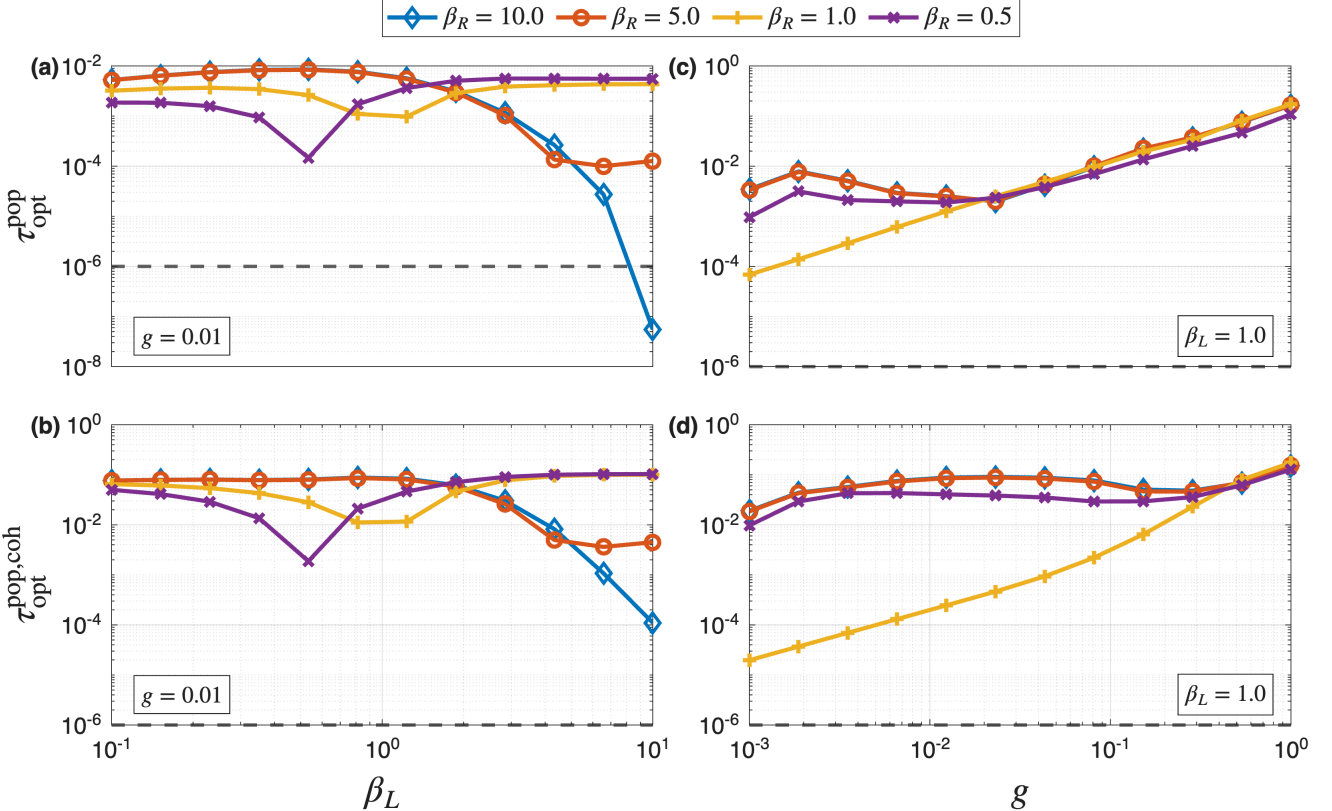


FIG. A1. Plots for $N_L = N_R = 1, N_M = 2$ (i.e. single qubit attached to left and right baths, see Sec. III A) for the isotropic XXZ Hamiltonian [Eq. (35)] keeping $\gamma_\ell = 1 \forall \ell$, $\omega_c = 10$ [Eq. (42)], $\epsilon_0 = 0.01$ [App. C], and $\beta_R = 10.0$ (blue diamond), 5.0 (red circle), 1.0 (yellow cross), 0.5 (purple plus). The black dashed horizontal line represents $\delta_{\text{tol}} = 10^{-6}$. (a) $\tau_{\text{opt}}^{\text{pop}}$ [Eq. (29)] versus β_L with $g = 0.01$. (b) $\tau_{\text{opt}}^{\text{pop,coh}}$ [Eq. (33)] versus β_L with $g = 0.01$. (c) $\tau_{\text{opt}}^{\text{pop}}$ versus g for $\beta_L = 1.0$. (d) $\tau_{\text{opt}}^{\text{pop,coh}}$ versus g for $\beta_L = 1.0$. This figure shows that we can never obtain even the correct leading-order populations (implying incorrect leading-order coherences as well) with only a single qubit attached at left and right baths.

given in Eq. (23). We have from Eq. (14),

$$\langle E_k | \mathcal{L}_2(\rho_{\text{NESS}}^{(0)}) | E_k \rangle = 0 \quad \forall k \quad (\text{B2})$$

Also, from the solution to the optimization problem, we know that

$$\sum_k |\langle E_k | \mathcal{L}_2'(\rho_{\text{NESS}}^{(0)}) | E_k \rangle| \geq \tau_{\text{opt}}^{\text{pop}}, \quad (\text{B3})$$

which implies, after substituting $\rho_{\text{NESS}}^{(0)}$ using Eq. (A1),

$$\sum_k \left| \sum_a p_a \langle E_k | \mathcal{L}_2'(|E_a\rangle \langle E_a|) | E_k \rangle \right| \geq \tau_{\text{opt}}^{\text{pop}}. \quad (\text{B4})$$

Let us define a matrix C such that its elements are given by

$$C_{ka} := \langle E_k | \mathcal{L}_2'(|E_a\rangle \langle E_a|) | E_k \rangle. \quad (\text{B5})$$

We can then rewrite Eq. (B4), using $b_k := \sum_a C_{ka} p_a$, as

$$\|C\mathbf{p}\|_1 = \sum_k \left| \sum_a C_{ka} p_a \right| = \sum_k |b_k| \geq \tau_{\text{opt}}^{\text{pop}}, \quad (\text{B6})$$

where the subscript 1 in the L.H.S. denotes the L_1 norm. Eq. (B6) can be compactly written as

$$\|C\mathbf{p}\|_1 = \|\mathbf{b}\|_1, \quad \mathbf{p} = (\{p_a\})^T, \quad (\text{B7})$$

where $\mathbf{b} = (\{b_k\})^T$. In the same manner taking $\mathbf{p}' =$

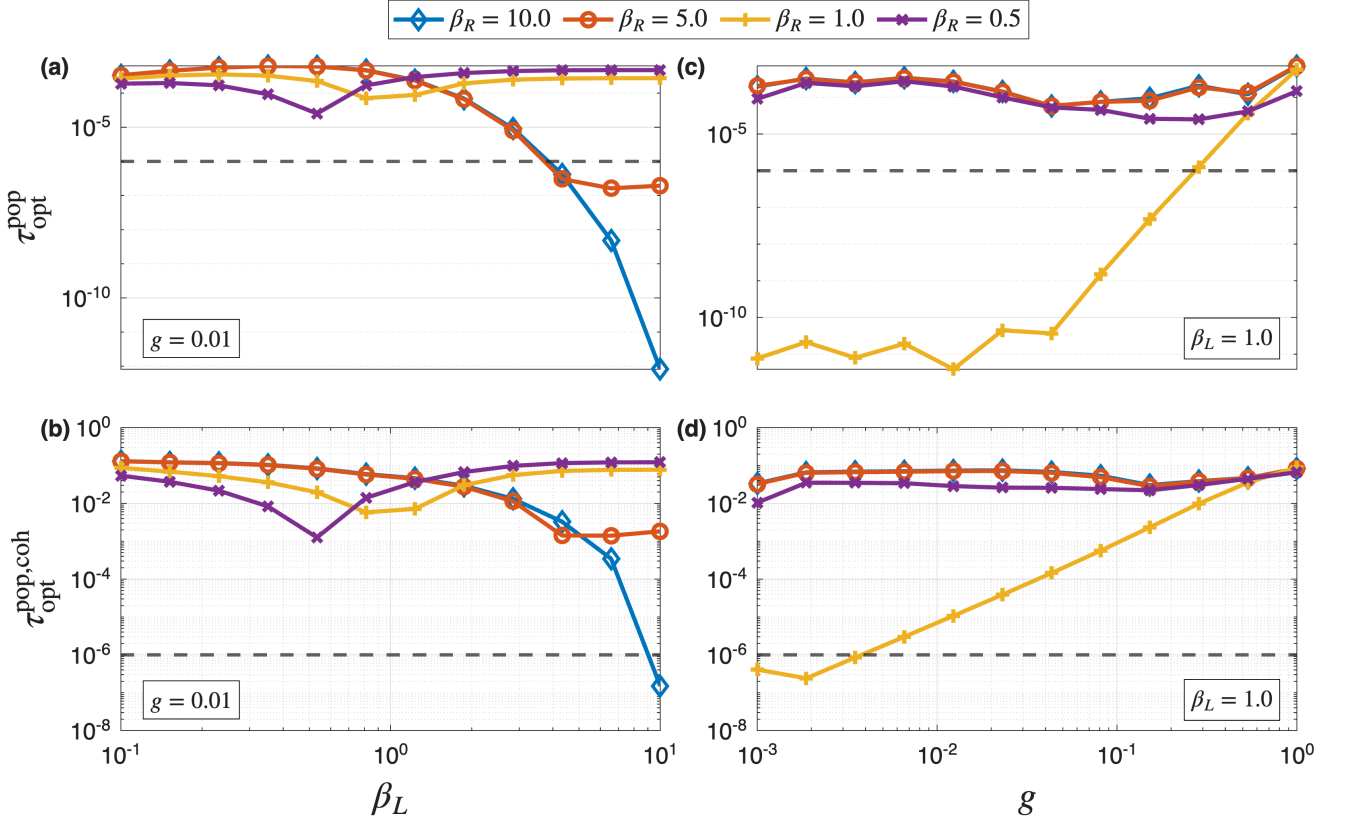


FIG. A2. Plots for $N_L = N_R = 2$, $N_M = 2$ for the isotropic XXZ Hamiltonian [Eq. (35)] keeping $\gamma_\ell = 1 \forall \ell$, $\omega_c = 10$ [Eq. (42)], $\epsilon_0 = 0.01$ [App. C], and $\beta_R = 10.0$ (blue diamond), 5.0 (red circle), 1.0 (yellow cross), 0.5 (purple plus). (a) $\tau_{\text{opt}}^{\text{pop}}$ [Eq. (29)] versus β_L with $g = 0.01$. (b) $\tau_{\text{opt}}^{\text{pop},\text{coh}}$ [Eq. (33)] versus β_L with $g = 0.01$. (c) $\tau_{\text{opt}}^{\text{pop}}$ versus g for $\beta_L = 1.0$. (d) $\tau_{\text{opt}}^{\text{pop},\text{coh}}$ versus g for $\beta_L = 1.0$. This figure shows that for a system with a small bias for onsite energies, even correct leading-order populations are unattainable in a wide parameter regime (implying incorrect leading-order coherences in these regimes as well).

$(\{p'_a\})^T$, we see that

$$\mathcal{L}'_2(\bar{\rho}_{\text{NESS}}^{(0)}) = 0 \implies C\mathbf{p}' = 0. \quad (\text{B8})$$

Our central question can now be reformulated as finding the upper and lower bounds on the quantity $\|\mathbf{p} - \mathbf{p}'\|_1$, given that $\|C\mathbf{p}\|_1 \geq \tau_{\text{opt}}^{\text{pop}}$, $C\mathbf{p}' = 0$, with \mathbf{p} , \mathbf{p}' being probability vectors. It is important to emphasize that this expression ($\|\mathbf{p} - \mathbf{p}'\|_1$) is identical to the trace distance between the two diagonal density matrices $\rho_{\text{NESS}}^{(0)} = \sum_a p_a |E_a\rangle\langle E_a|$ and $\bar{\rho}_{\text{NESS}}^{(0)} = \sum_a p'_a |E_a\rangle\langle E_a|$.

We now utilize the triangle inequality, to show that for any vector \mathbf{l} , we have

$$\begin{aligned} \|Cl\|_1 &= \sum_k \left| \sum_a C_{ka} l_a \right| \\ &\leq \sum_a \sum_k (|l_a C_{ka}|) \\ &= \sum_a \left(|l_a| \sum_k |C_{ka}| \right). \end{aligned} \quad (\text{B9})$$

The inner sum $\sum_k |C_{ka}|$ in the RHS of Eq. (B9) corre-

sponds to the total “weight” applied by the matrix C to each component $|l_a\rangle$. Let us define a constant α which bounds $\sum_k |C_{ka}|$ as

$$\sum_k |C_{ka}| \leq \alpha. \quad (\text{B10})$$

Now, substituting $\mathbf{l} = \mathbf{p} - \mathbf{p}'$ and noting that $C\mathbf{p}' = 0$, $\|C\mathbf{p}\|_1 \geq \tau_{\text{opt}}^{\text{pop}}$, we have from Eqs. (B9) and (B10)

$$\begin{aligned} \|\mathbf{p} - \mathbf{p}'\|_1 &\geq \|C(\mathbf{p} - \mathbf{p}')\|/\alpha \\ &= \|C\mathbf{p}\|/\alpha \\ &\geq \tau_{\text{opt}}^{\text{pop}}/\alpha. \end{aligned} \quad (\text{B11})$$

The only thing left to do in our proof is to find an explicit form of the upper bound α . We will do so with some straightforward algebra. Given that \mathcal{L}'_2 contains $\Gamma^{(L)}$ and $\Gamma^{(R)}$ [Eq. (23)], we have

$$\begin{aligned}
C_{ka} &= \langle E_k | \mathcal{L}'_2(|E_a\rangle\langle E_a|) |E_k\rangle \\
&= \sum_{ij}^{d_L^2-1} \frac{\Gamma_{ij}^{(L)}}{2^{(N_M+N_R)}} (\langle E_k | (f_i \otimes I_{MR}) |E_a\rangle\langle E_a| (f_j \otimes I_{MR})^\dagger |E_k\rangle - \langle E_k | (f_i \otimes I_{MR})^\dagger (f_j \otimes I_{MR}) |E_k\rangle \delta_{ka}) \\
&+ \sum_{ij}^{d_R^2-1} \frac{\Gamma_{ij}^{(R)}}{2^{(N_M+N_R)}} (\langle E_k | (I_{LM} \otimes f_i) |E_a\rangle\langle E_a| (I_{LM} \otimes f_j)^\dagger |E_k\rangle - \langle E_k | (I_{LM} \otimes f_i)^\dagger (I_{LM} \otimes f_j) |E_k\rangle \delta_{ka}) \quad (B12)
\end{aligned}$$

The H_{LS} terms in Eq. (23) do not contribute as they are Hermitian and hence cancel off after expanding the commutator. To analyze Eq. (B12) further, we concentrate only on the term with the left bath sum (second line in Eq. (B12)). A similar following analysis also holds for the right bath sum (third line in Eq. (B12)). We define

$$m_{ka}^i = \langle E_k | (f_i \otimes I_{MR}) |E_a\rangle. \quad (B13)$$

The elements m_{ka}^i are just the value at the (k, a) position of the matrix $m^i := f_i \otimes I_{MR}$ in the energy eigenbasis. The idea now is to find the operator norm of m^i (denoted by $\|m^i\|$) and use the fact that the absolute value of a matrix element in an orthonormal basis is bounded by the operator norm of the matrix [54]. In other words, we

use the fact that

$$|m_{ka}^i| \leq \|m^i\|. \quad (B14)$$

The operator norm of a matrix is simply the largest absolute value of the singular values of matrix, and the matrices in m^i are tensor products of simpler, smaller matrices. In particular, we have $\|-\sigma_z/\sqrt{2}\| = \|I_2/\sqrt{2}\| = 1/\sqrt{2}$, and $\|\sigma_+\| = \|\sigma_-\| = 1$. Now, f_i is a tensor product over different basis operators, that is $f_i \in \{-\sigma_z/\sqrt{2}, \sigma_+, \sigma_-, I_2/\sqrt{2}\}^{\otimes N_L}$. Using the fact that $\|A \otimes B\| = \|A\| \|B\|$, and Eq. (B14), we obtain

$$|m_{ka}^i| \leq \|m^i\| \leq 1. \quad (B15)$$

A similar analysis holds for the right bath, which we denote using m' instead of m . Iteratively applying triangle inequalities on Eq. (B12), alongside our modified notation, gives us

$$\begin{aligned}
\sum_k |C_{ka}| &= \sum_k \left| \sum_{ij} \frac{\Gamma_{ij}^{(L)}}{2^{(N_M+N_R)}} \left(m_{ka}^i (m_{ka}^j)^\dagger - \sum_n (m_{nk}^i)^\dagger m_{nk}^j \delta_{ka} \right) + \frac{\Gamma_{ij}^{(R)}}{2^{(N_M+N_L)}} \left(m_{ka}^i (m_{ka}^j)^\dagger - \sum_n (m_{nk}^i)^\dagger m_{nk}^j \delta_{ka} \right) \right| \\
&\leq \sum_k \sum_{ij} \frac{|\Gamma_{ij}^{(L)}|}{2^{(N_M+N_R)}} \left(|m_{ka}^i (m_{ka}^j)^\dagger| + \sum_n |(m_{nk}^i)^\dagger m_{nk}^j| \delta_{ka} \right) + \frac{|\Gamma_{ij}^{(R)}|}{2^{(N_M+N_L)}} \left(|m_{ka}^i (m_{ka}^j)^\dagger| + \sum_n |(m_{nk}^i)^\dagger m_{nk}^j| \delta_{ka} \right) \\
&\leq \left(\sum_{ij} |\Gamma_{ij}^{(L)}| \left(\frac{d_L}{d} \right) \sum_k (1 + d\delta_{ka}) + \sum_{ij} |\Gamma_{ij}^{(R)}| \left(\frac{d_R}{d} \right) \sum_k (1 + d\delta_{ka}) \right) \\
&= 2 \left(\sum_{ij} |\Gamma_{ij}^{(L)}| d_L + \sum_{ij} |\Gamma_{ij}^{(R)}| d_R \right) \quad (B16)
\end{aligned}$$

where $d_L = 2^{N_L}$, $d_R = 2^{N_R}$, $d_M = 2^{N_M}$, $d = d_L d_M d_R$. Here, we used Eq. (B15) in the third line. For the fourth line, we use the fact that $\Gamma_{ij}^{(L)}$, $\Gamma_{ij}^{(R)}$ are positive semi-definite matrices with trace values t_L and t_R respectively: we can utilize the fact that the sum of the absolute value of matrix elements of such matrices is upper bounded by their dimensionality [54], i.e.

$\sum_{ij} |\Gamma_{ij}^{(L)}| \leq t_L (d_L^2 - 1)$, $\sum_{ij} |\Gamma_{ij}^{(R)}| \leq t_R (d_R^2 - 1)$. Recall that $\Gamma_{ij}^{(L)}$ is a $d_L^2 - 1$ dimensional matrix and similarly $\Gamma_{ij}^{(R)}$ is a $d_R^2 - 1$ dimensional matrix. Thus, we have from

Eq. (B16) that

$$\sum_k |C_{ka}| \leq 2(t_L d_L^3 + t_R d_R^3 - t_L d_L - t_R d_R) \quad (B17)$$

Hence, comparing Eq. (B17) with Eq. (B10), we can set $\alpha = 2(t_L d_L^3 + t_R d_R^3 - t_L d_L - t_R d_R)$ and arrive at Eq. (31) as quoted in the main text. This concludes our proof. \square

Appendix C: Numerical results for non-zero energy bias in half of the chain.

We recall that in the main text, we presented numerical results for zero energy bias, i.e. the onsite energy ω_0 present in Eq. (35) was same for all sites in Figs. 2 and 3. Here we introduce a dimensionless parameter which we call the energy bias ϵ_0 , where $\omega_0^{(\ell)} = 1$ for ℓ between 1 and $N/2$ and $\omega_0^{(\ell)} = 1 + \epsilon_0$ for the rest. To emphasize the generality of our findings presented in

Secs. III A and III B, in this appendix, we discuss the case of non-zero energy bias.

Figs. A1(a,b,c,d) highlight plots for the isotropic XXZ Hamiltonian for a single qubit attached to the left and right baths ($N_L = N_R = 1$) respectively with a non-zero bias of $\epsilon_0 = 0.01$. Correct populations may only be possible in the equilibrium ($\beta_L = \beta_R$) scenario, while correct populations and coherences together are not possible in neither equilibrium nor non-equilibrium ($\beta_L \neq \beta_R$) setups over the parameter regimes presented in the plots. Figs. A2(a,b,c,d) highlight the same type of plots but with two qubits attached to the left and right baths ($N_L = N_R = 2$). Here, correct populations may be possible but only for a very small range of values in the non-equilibrium setup as opposed to the much larger parameter range in the zero bias case $\epsilon_0 = 0$ [see Fig. 3(a)]. Correct populations and coherences together are still not possible for non-equilibrium setup, but maybe possible in the equilibrium scenario for very low inter-site coupling strength.

[1] H.-P. Breuer and F. Petruccione, *The Theory of Open Quantum Systems* (Oxford University Press, Oxford, 2006).

[2] H. Carmichael, *Statistical Methods in Quantum Optics 1. Master Equations and Fokker-Planck Equations* (Springer-Verlag Berlin Heidelberg, 2002).

[3] Á. Rivas and S. F. Huelga, *Open Quantum Systems: An Introduction* (Springer, 2012).

[4] F. Campaioli, J. H. Cole, and H. Hapuarachchi, Quantum master equations: Tips and tricks for quantum optics, quantum computing, and beyond, *PRX Quantum* **5**, 020202 (2024).

[5] M. Stefanini, A. A. Ziolkowska, D. Budker, U. Poschinger, F. Schmidt-Kaler, A. Browaeys, A. Imamoglu, D. Chang, and J. Marino, Is lindblad for me?, *arXiv* (2025), 2506.22436 [quant-ph].

[6] H. M. Wiseman and G. J. Milburn, *Quantum measurement and control* (Cambridge university press, 2009).

[7] D. Walls and G. J. Milburn, *Quantum optics* (Springer-Verlag Berlin Heidelberg, 2008).

[8] M. A. Nielsen and I. L. Chuang, *Quantum computation and quantum information* (Cambridge university press, 2010).

[9] S. Hacohen-Gourgy and L. S. Martin, Continuous measurements for control of superconducting quantum circuits, *Advances in Physics: X* **5**, 1813626 (2020).

[10] J. Gambetta, A. Blais, M. Boissonneault, A. A. Houck, D. I. Schuster, and S. M. Girvin, Quantum trajectory approach to circuit qed: Quantum jumps and the zeno effect, *Phys. Rev. A* **77**, 012112 (2008).

[11] H. J. Carmichael, Quantum trajectory theory for cascaded open systems, *Phys. Rev. Lett.* **70**, 2273 (1993).

[12] V. Gorini, A. Kossakowski, and E. C. G. Sudarshan, Completely positive dynamical semigroups of n-level systems, *Journal of Mathematical Physics* **17**, 821 (1976).

[13] G. Lindblad, On the generators of quantum dynamical semigroups, *Commun. Math. Phys.* **48**, 119 (1976).

[14] F. Bloch, Generalized theory of relaxation, *Phys. Rev.* **105**, 1206 (1957).

[15] A. G. Redfield, On the theory of relaxation processes, *IBM Journal of Research and Development* **1**, 19 (1957).

[16] A. Suárez, R. Silbey, and I. Oppenheim, Memory effects in the relaxation of quantum open systems, *The Journal of Chemical Physics* **97**, 5101 (1992).

[17] S. Gnutzmann and F. Haake, Positivity violation and initial slips in open systems, *Zeitschrift für Physik B Condensed Matter* **101**, 263 (1996).

[18] R. Hartmann and W. T. Strunz, Accuracy assessment of perturbative master equations: Embracing nonpositivity, *Phys. Rev. A* **101**, 012103 (2020).

[19] D. Tupkary, A. Dhar, M. Kulkarni, and A. Purkayastha, Searching for lindbladians obeying local conservation laws and showing thermalization, *Physical Review A* **107**, 062216 (2023).

[20] A. Rivas, A. D. K. Plato, S. F. Huelga, and M. B. Plenio, Markovian master equations: a critical study, *New Journal of Physics* **12**, 113032 (2010).

[21] A. S. Trushechkin and I. V. Volovich, Perturbative treatment of inter-site couplings in the local description of open quantum networks, *EPL (Europhysics Letters)* **113**, 30005 (2016).

[22] G. Deçordi and A. Vidiella-Barranco, Two coupled qubits interacting with a thermal bath: A comparative study of different models, *Optics Communications* **387**, 366 (2017).

[23] G. Kiršanskas, M. Franckie, and A. Wacker, Phenomenological position and energy resolving lindblad approach to quantum kinetics, *Phys. Rev. B* **97**, 035432 (2018).

[24] M. Cattaneo, G. L. Giorgi, S. Maniscalco, and R. Zambrini, Local versus global master equation with common and separate baths: superiority of the global approach in partial secular approximation, *New Journal of Physics*

21, 113045 (2019).

[25] D. Davidović, Completely positive, simple, and possibly highly accurate approximation of the redfield equation, *Quantum* **4**, 326 (2020).

[26] E. Mozgunov and D. Lidar, Completely positive master equation for arbitrary driving and small level spacing, *Quantum* **4**, 227 (2020).

[27] G. McCauley, B. Cruikshank, D. I. Bondar, and K. Jacobs, Accurate lindblad-form master equation for weakly damped quantum systems across all regimes, *npj Quantum Information* **6** (2020).

[28] E. Kleinherbers, N. Szpak, J. König, and R. Schützhold, Relaxation dynamics in a hubbard dimer coupled to fermionic baths: Phenomenological description and its microscopic foundation, *Phys. Rev. B* **101**, 125131 (2020).

[29] D. Davidović, Geometric-arithmetic master equation in large and fast open quantum systems, *Journal of Physics A: Mathematical and Theoretical* **55**, 455301 (2022).

[30] A. S. Trushechkin, M. Merkli, J. D. Cresser, and J. Anders, Open quantum system dynamics and the mean force gibbs state, *AVS Quantum Science* **4**, 012301 (2022).

[31] S. Scali, J. Anders, and L. A. Correa, Local master equations bypass the secular approximation, *Quantum* **5**, 451 (2021).

[32] T. Becker, L.-N. Wu, and A. Eckardt, Lindbladian approximation beyond ultraweak coupling, *Phys. Rev. E* **104**, 014110 (2021).

[33] A. Schnell, Global becomes local: Efficient many-body dynamics for global master equations, *Phys. Rev. Lett.* **134**, 250401 (2025).

[34] D. Tupkary, A. Dhar, M. Kulkarni, and A. Purkayastha, Fundamental limitations in lindblad descriptions of systems weakly coupled to baths, *Phys. Rev. A* **105**, 032208 (2022).

[35] C. H. Fleming and N. I. Cummings, Accuracy of perturbative master equations, *Phys. Rev. E* **83**, 031117 (2011).

[36] L. Vandenberghe and S. Boyd, Semidefinite programming, *SIAM Review* **38**, 49 (1996), <https://doi.org/10.1137/1038003>.

[37] M. M. Wolf, J. Eisert, T. S. Cubitt, and J. I. Cirac, Assessing non-markovian quantum dynamics, *Phys. Rev. Lett.* **101**, 150402 (2008).

[38] T. S. Cubitt, J. Eisert, and M. M. Wolf, The complexity of relating quantum channels to master equations, *Communications in Mathematical Physics* **310**, 383 (2012).

[39] A. H. Kiilerich and K. Mølmer, Multistate and multi-hypothesis discrimination with open quantum systems, *Phys. Rev. A* **97**, 052113 (2018).

[40] Á. Rivas and S. F. Huelga, Open quantum systems, *SpringerBriefs in Physics* (2012).

[41] C. Fleming, A. Roura, and B. Hu, Exact analytical solutions to the master equation of quantum brownian motion for a general environment, *Annals of Physics* **326**, 1207–1258 (2010).

[42] R. S. Whitney, Staying positive: going beyond lindblad with perturbative master equations, *Journal of Physics a Mathematical and Theoretical* **41**, 175304 (2008).

[43] M. Grant and S. Boyd, CVX: Matlab software for disciplined convex programming, version 2.1, <http://cvxr.com/cvx> (2014).

[44] A. Purkayastha, A. Dhar, and M. Kulkarni, Out-of-equilibrium open quantum systems: A comparison of approximate quantum master equation approaches with exact results, *Phys. Rev. A* **93**, 062114 (2016).

[45] G. Guarneri, M. Kolář, and R. Filip, Steady-state coherences by composite system-bath interactions, *Phys. Rev. Lett.* **121**, 070401 (2018).

[46] M. Žnidarič, Spin transport in a one-dimensional anisotropic heisenberg model, *Physical review letters* **106**, 220601 (2011).

[47] M. Žnidarič, Transport in a one-dimensional isotropic heisenberg model at high temperature, *Phys. Rev. E* **92**, 042143 (2015).

[48] T. Prosen and M. Žnidarič, Matrix product simulations of non-equilibrium steady states of quantum spin chains, *Journal of Statistical Mechanics: Theory and Experiment* **2009**, P02035 (2009).

[49] J. T. Barreiro, M. Müller, P. Schindler, D. Nigg, T. Monz, M. Chwalla, M. Hennrich, C. F. Roos, P. Zoller, and R. Blatt, An open-system quantum simulator with trapped ions, *Nature* **470**, 486 (2011).

[50] P. Schindler, M. Müller, D. Nigg, J. T. Barreiro, E. A. Martinez, M. Hennrich, T. Monz, S. Diehl, P. Zoller, and R. Blatt, Quantum simulation of dynamical maps with trapped ions, *Nature Physics* **9**, 361 (2013).

[51] G. García-Pérez, M. A. C. Rossi, and S. Maniscalco, Ibm q experience as a versatile experimental testbed for simulating open quantum systems, *npj Quantum Information* **6**, 1 (2020).

[52] C. W. Kim, J. M. Nichol, A. N. Jordan, and I. Franco, Analog quantum simulation of the dynamics of open quantum systems with quantum dots and microelectronic circuits, *PRX Quantum* **3**, 040308 (2022).

[53] S. Sarma, <https://github.com/lo5681os/LimitationLindbladians> (2025).

[54] R. A. Horn and C. R. Johnson, *Matrix Analysis*, 2nd ed. (Cambridge University Press, Cambridge, 2012).